



**HAL**  
open science

## Induction of a non-apoptotic mode of cell death associated with autophagic characteristics with steroidal maleic anhydrides and $7\beta$ -hydroxycholesterol on glioma cells

K. Sassi, T. Nury, A. Zarrouk, R. Sghaier, A. Khalafi-Nezhad, A. Vejux, M. Samadi, F. Ben Aissa-Fennira, G. Lizard

### ► To cite this version:

K. Sassi, T. Nury, A. Zarrouk, R. Sghaier, A. Khalafi-Nezhad, et al.. Induction of a non-apoptotic mode of cell death associated with autophagic characteristics with steroidal maleic anhydrides and  $7\beta$ -hydroxycholesterol on glioma cells. *Journal of Steroid Biochemistry and Molecular Biology*, 2019, 191, pp.105371. 10.1016/j.jsbmb.2019.04.020 . hal-03485843

**HAL Id: hal-03485843**

**<https://hal.science/hal-03485843>**

Submitted on 20 Dec 2021

**HAL** is a multi-disciplinary open access archive for the deposit and dissemination of scientific research documents, whether they are published or not. The documents may come from teaching and research institutions in France or abroad, or from public or private research centers.

L'archive ouverte pluridisciplinaire **HAL**, est destinée au dépôt et à la diffusion de documents scientifiques de niveau recherche, publiés ou non, émanant des établissements d'enseignement et de recherche français ou étrangers, des laboratoires publics ou privés.



Distributed under a Creative Commons Attribution - NonCommercial 4.0 International License

## **Induction of a non-apoptotic mode of cell death associated with autophagic characteristics with steroidal maleic anhydrides and 7 $\beta$ -hydroxycholesterol on glioma cells**

K. Sassi <sup>a,b #</sup>, T. Nury <sup>a #</sup>, A. Zarrouk <sup>c</sup>, R. Sghaier <sup>a,c,d</sup>, A. Khalafi-Nezhad <sup>e</sup>, A. Vejux <sup>a</sup>, M. Samadi <sup>f,\*</sup>, F. Ben Aissa-Fennira <sup>b</sup>, G. Lizard <sup>a,\*</sup>

<sup>a</sup> Univ. Bourgogne Franche-Comté, Team ‘Biochemistry of the peroxisome, inflammation and lipid metabolism’ EA 7270 / Inserm, Dijon, France

<sup>b</sup> Univ. Tunis El Manar, Laboratory of Onco-Hematology (LR05ES05), Faculty of Medicine, Tunis, Tunisia

<sup>c</sup> Univ. Monastir, Lab-NAFS ‘Nutrition - Functional Food & Vascular Health’ (LR12ES05), Monastir, & Faculty of Medicine, Laboratory of Biochemistry, Sousse, Tunisia

<sup>d</sup> Univ. Manouba, Laboratory of Biotechnology and Valorisation of Bio-Geo Ressources, Higher Institute of Biotechnology (LR11ES31), Sidi Thabet, Tunisia

<sup>e</sup> Dept. of Chemistry, College of Sciences, Shiraz University, Shiraz, Iran

<sup>f</sup> LCPMC-A2, ICPM, Dept of Chemistry, Univ. Lorraine, Metz Technopôle, Metz, France

\* To whom correspondence should be sent:

- *Chemistry*: Prof. Mohammad Samadi, LCPMC-A2, ICPM, Département de Chimie, Université de Lorraine, Metz Technopôle, 57 000 Metz, France

Phone : +33 387 54 77 93; E.mail : mohammad.samadi@univ-lorraine.fr

-*Biology*: Dr Gérard Lizard, Univ. Bourgogne Franche-Comté / Equipe Bio-peroxIL (EA 7270) / Inserm, Faculté des Sciences Gabriel, 6 Bd Gabriel, 21 000 Dijon, France

Phone: +33 380 39 62 56; Fax: +33 380 39 62 50; Email: Gerard.Lizard@u-bourgogne.fr

# : Sassi K and Nury T equally contributed.

**Abstract**

Steroidal maleic anhydrides were prepared in one step: lithocholic, chenodeoxicholic, deoxicholic, ursocholic, and hyodeoxicholic acid derivatives. Their capability to induce cell death was studied on C6 rat glioma cells, and 7 $\beta$ -hydroxycholesterol was used as positive cytotoxic control. The highest cytotoxicity was observed with lithocholic and chenodeoxicholic acid derivatives (23-(4-methylfuran-2,5-dione)-3 $\alpha$ -hydroxy-24-nor-5 $\beta$ -cholane (compound 1a), and 23-(4-methylfuran-2,5-dione)-3 $\alpha$ ,7 $\alpha$ -dihydroxy-24-nor-5 $\beta$ -cholane (compound 1b), respectively), which induce a non-apoptotic mode of cell death associated with mitochondrial membrane potential loss and reactive oxygen species overproduction. No cells with condensed and/or fragmented nuclei, no PARP degradation and no cleaved-caspase-3, which are apoptotic criteria, were observed. Similar effects were found with 7 $\beta$ -hydroxycholesterol. The cell clonogenic survival assay showed that compound 1b was more cytotoxic than compound 1a and 7 $\beta$ -hydroxycholesterol. Compound 1b and 7 $\beta$ -hydroxycholesterol also induce cell cycle modifications. In addition, compounds 1a and 1b, and 7 $\beta$ -hydroxycholesterol favour the formation of large acidic vacuoles revealed by staining with acridine orange and monodansylcadaverine evocating autophagic vacuoles; they also induce an increased ratio of [LC3-II / LC3-I], and modify the expression of mTOR, Beclin-1, Atg12, and Atg5-Atg12 which are autophagic criteria. The ratio [LC3-II / LC3-I] is also strongly modified by bafilomycin acting on the autophagic flux. Rapamycin, an autophagic inducer, and 3-methyladenine, an autophagic inhibitor, reduce and increase 7 $\beta$ -hydroxycholesterol-induced cell death, respectively, supporting that 7 $\beta$ -hydroxycholesterol induces survival autophagy. Alpha-tocopherol also strongly attenuates 7 $\beta$ -hydroxycholesterol-induced cell death. However, rapamycin, 3-methyladenine, and  $\alpha$ -tocopherol have no effect on compounds 1a and 1b-induced cell death. It is concluded that these compounds trigger a non apoptotic mode of cell death, involving the mitochondria and associated with several characteristics of autophagy.

**Keywords**, C6 rat glioma cells, steroidal maleic anhydrides, 7 $\beta$ -hydroxycholesterol, cell death, autophagy.

## 1. Introduction

Steroids derive from cholesterol and have several biological activities. They may have beneficial or detrimental effects on health, and some of them or their derivatives may be of interest for the treatment of cancer [1, 2]. For example, dendrogenin A, a steroidal alkaloid identified in humans, which arises from the stereo selective enzymatic conjugation of 5,6 $\alpha$ -epoxycholesterol (5,6 $\alpha$ -EC) with histamine, induces the re-differentiation of cancer cells in vitro and in vivo and prevents breast cancer and melanoma development in mice [3, 4]. Bile acids are steroid molecules and the products of cholesterol catabolism; they are synthesized in the liver and excreted in the digestive tract [1, 5]. It has been established that bile acids have anti-neoplastic and anti-carcinogenic properties on several cancer cell models, such as tamoxifen-resistant breast cancer, colon cancer, prostate cancer and neuroblastoma [2]. Bile acids are flexible building blocks for numerous synthetic applications. A number of studies have described the conjugation of active substances with bile derivatives at the 3- and 24-positions of the steroid nucleus and side chains. This strategy is efficient to generate new conjugated or hybrid bile acids with potent anti-proliferative and apoptotic properties on several tumor cells [2]. A number of natural products or derivatives such as tautomycin, tautomycetin, and chaetomelic acid, which contain a substituted maleic anhydride unit, have been described. These compounds have a wide range of biological activities including enzymatic inhibitory effects such as anti-farnesyltransferase activities blocking Ras processing, which could contribute to their anti-tumor properties [6, 7, 8]. Based on structure–activity studies, the maleic anhydride moiety is required for the bioactivity [8].

At the moment, little progress has been made in the treatment of glioblastoma, which is considered the most lethal brain cancer. Malignant gliomas are the most common primary tumors of the brain, and represent around 78% of these tumors [9]. According to the World Health Organization, gliomas have been classified into four histologic grades, and glioblastoma multiform (grade IV) is the most malignant form showing an average survival

rate of 9-12 months [10]. Overall, long-term survival of glioblastoma is rare, and several variables beside tumor size and location determine a patient's chances survival: age at diagnosis, functional status, histologic and genetic markers [11]. Cytotoxic therapy, including steroids, monoclonal antibodies and radiation, is most often used but its efficacy is limited [12, 13, 14, 15, 16]. Therefore, for this aggressive form of brain cancer, there is a real need to identify new drugs. As there is evidence that sex hormones, which are derived from cholesterol and have a steroid structure, can regulate the development of brain tumors there is a rationale to use molecules that include a steroid structure for the treatment of gliomas [17]. Up to now, steroids are used to reduce tumor swelling and to decrease pressure inside the head. However, no steroid compounds with anti-tumor activities are used even though there is some evidence that natural and semi-synthetic steroids have lipotoxic and anti-cancer activities on various models, including colon and prostate cancer cells [2, 18, 19, 20]. It has also been reported that 7 $\beta$ -hydroxycholesterol (7 $\beta$ -OHC) has anti-proliferative and cytotoxic effects against C6 rat glioma cells [21, 22], and that 7 $\beta$ -hydroxycholesteryl-3 $\beta$ (ester)-oleate and 7 $\beta$ -hydroxycholesteryl-3- $\beta$ -O(ether)-oleyl have anti-tumor activities against glioblastomas induced by C6 cells in rat brain cortex [23]. Since steroids can pass the blood brain barrier, and as some of them, such as oxysterols, have anti-tumor activities, they are attractive molecules to develop new anti-tumor drugs against aggressive brain cancers, such as glioma.

In the present study, steroidal maleic anhydrides were obtained by the Barton decarboxylation reaction using thiohydroxamic esters as a source of carbon radicals [24, 25, 26, 27, 28]. The cytotoxic activities of the maleic anhydrides obtained were characterized on C6 rat glioma cells [29, 30]. We previously reported that some of these steroidal maleic anhydrides were potent inducers of cell death on C6 cells [31]. So, we attempted to determine the type of cell

death triggered by these steroidal maleic anhydrides and by 7 $\beta$ -OHC (used as positive lipotoxic / cytotoxic oxysterol) on C6 cells.

## 2. Materials and Methods

### 2.1 Chemical Synthesis

The chemical synthesis of compounds 1a (23-(4-methylfuran-2,5-dione)-3 $\alpha$ -hydroxy-24-nor-5 $\beta$ -cholane), 1b (23-(4-methylfuran-2,5-dione)-3 $\alpha$ ,7 $\alpha$ -dihydroxy-24-nor-5 $\beta$ -cholane), 1c (23-(4-methylfuran-2,5-dione)-3 $\alpha$ ,12 $\alpha$ -dihydroxy-24-nor-5 $\beta$ -cholane), 1d (23-(4-methylfuran-2,5-dione)-3 $\alpha$ ,7 $\beta$ -dihydroxy-24-nor-5 $\beta$ -cholane), and 1e (23-(4-methylfuran-2,5-dione)-3 $\alpha$ ,6 $\alpha$ -dihydroxy-24-nor-5 $\beta$ -cholane) was realized as previously described [31] (**Fig. 1**).

### 2.2 Cell culture and treatments

C6 rat glioma cells were seeded at 240,000 cells per well in 6-well microplates containing 2 mL of culture medium (Dulbecco's modified Eagle medium (DMEM) (Lonza) supplemented with 10% (v/v) heat-inactivated foetal bovine serum (FBS) (Pan Biotech) and 1% antibiotics (100 U/mL penicillin, 100 mg/mL streptomycin) (Pan Biotech)). C6 cells were incubated at 37°C in a humidified atmosphere containing 5% CO<sub>2</sub>, and passaged twice a week. At each passage, cells were trypsinized with a (0.05% trypsin - 0.02% EDTA) solution (Pan Biotech). The conditions of treatment of C6 cells with the different compounds (lithocholic, chenodeoxycholic, deoxycholic, ursolic, and hyodeoxycholic acid derivatives (compounds 1a, 1b, 1c, 1d, 1e, respectively) (**Fig. 1**)) and 7 $\beta$ -OHC (lipotoxic compound / cytotoxic oxysterol used as positive reference) were the following: initial concentrations of chenodeoxycholic (1b; Molecular Weight (MW): 458.3031), deoxycholic (1c; MW: 458.3032), ursolic (1d; MW: 458.3031), and hyodeoxycholic (1e; MW: 458.3035) acid derivatives were prepared at 800  $\mu$ g/mL (1 mg of compound with 50  $\mu$ L absolute ethanol; dilution 1/25 in culture medium to obtain a stock solution of 800  $\mu$ g/mL). The initial

concentration of lithocholic acid derivative (**1a**; MW: 442.3080) was prepared at 400 µg/mL (1 mg of compound with 100 µL absolute ethanol; dilution 1/25 in culture medium to obtain a stock solution of 400 µg/mL). After 24 h of culture, C6 cells were further treated for 24 h with various concentrations of these compounds: 2.5, 5, 10, 20, 40 and 80 µg/mL (range of concentrations: 5 to 160 µM). The stock solution of 7β-OHC (Sigma-Aldrich; MW: 402.65), used at 20-40 µg/mL (50-100 µM), was prepared at 800 µg/mL (1 mg of compound with 50 µL absolute ethanol; dilution 1/25 in culture medium to obtain a stock solution of 800 µg/mL) as previously described [32, 33, 34]. In the stock solutions, the maximal ethanol concentration was 4%. Thus, depending on the sterol concentration, the maximal ethanol concentration in the culture medium can reach 0.4% when the sterols were used at 80 µg/mL; the ethanol concentration was twice less (0.2%) or four less (0.1%) when the sterols were used at 40 or 20 µg/mL, respectively. Thus, in the different experiments, the control (untreated cells) was always compared to the vehicle control (ethanol) realized with the highest ethanol concentration introduced in the culture medium; therefore, the percentage of ethanol in the vehicle control depended on the maximal concentration of sterol used in the experiment. α-tocopherol (Sigma-Aldrich), prepared as previously described [34], was used at 500 µM and simultaneously added with compounds **1a**, **1b** or 7β-OHC. Bafilomycin (Bafilomycin A1: 100 nM final concentration) was added in the culture medium 20 h after the addition of compounds **1a**, **1b** or 7β-OHC (4 h before the end of the treatment). Rapamycin (rapa: 5 µM final concentration) (Sigma-Aldrich) and 3-methyladenine (3-MA: 15 mM final concentration) (Sigma-Aldrich) were simultaneously added with compounds **1a**, **1b** or 7β-OHC.

### ***2.3 Phase contrast microscopy***

Cell morphology (adherent and non-adherent cells) and cell density was observed after 24 h of culture on untreated and treated cells under an inverted-phase contrast microscope (Axiovert 40CFL, Zeiss) at x400 magnification. For each condition of culture, 9 fields in the center of the well were observed [35]. Digitized images were obtained with a video camera (AxioCam ICm1, Zeiss).

#### ***2.4 MTT assay***

The MTT assay was used to evaluate the effects of treatments on cell proliferation and/or mitochondrial activity [36]. The MTT assay was carried out on C6 cells plated in 6-well flat-bottom culture plates after 24 h of culture on untreated and treated cells. MTT salt (Sigma-Aldrich) is reduced to formazan in the metabolically active cells by the mitochondrial enzyme succinate dehydrogenase [37]. The plates were read at 570 nm with a microplate reader - Tecan Sunrise (Tecan).

#### ***2.5 Crystal violet staining assay***

The number of adherent cells was estimated by staining with crystal violet (Sigma-Aldrich). Cells were seeded in triplicate in 6-well plates and treated with the different compounds for 24 h. At the end of the treatment, cells were washed with PBS, stained with crystal violet (Sigma-Aldrich) for 5 min, and rinsed with water three times. Absorbance was read at 570 nm after extraction of the dye with 0.1 mol/L sodium citrate (Sigma-Aldrich) in 50% ethanol (Carlo-Erba). Data obtained with crystal violet staining (optical density per well) were expressed as % control (untreated cells).

#### ***2.6 Cell clonogenic survival assay***

Cell clonogenic survival assay or colony formation assay is an in vitro cell survival assay based on the ability of a single cell to grow into a colony following insult with chemicals or radiation [38, 39]. At the end of treatment in 6-well plates, cells were trypsinized, counted on a Malassez hemocytometer in the presence of trypan blue (v/v), and 1,000 living cells were cultured in a 100 mm Petri dish in 10 mL of culture medium for 6 days. Cells permeable to propidium iodide (PI: 1  $\mu\text{g}/\text{mL}$ ) corresponding either to dead cells or to cells with altered plasma membranes were determined by flow cytometry at the beginning of the culture (Day 0). After 6 days of culture, the cells were stained with crystal violet to visualize cell colonies; the medium was changed twice a week.

### ***2.7 Nuclear staining with Hoechst 33342***

Nuclear morphology of control (untreated cells), and treated cells was characterized by fluorescence microscopy after staining with Hoechst 33342 (Sigma-Aldrich) (2  $\mu\text{g}/\text{mL}$ ) [40]. Cell deposits of about 40,000 cells were applied to glass slides by cytocentrifugation (5 min, 1,500 rpm) with a cytospin 2 (Shandon), mounted in Dako fluorescent mounting medium (Dako) and stored in the dark at 4°C until observation. The morphological aspect of the cell nuclei was determined with an Axioskop fluorescent microscope (Zeiss). For each sample, 300 nuclei were examined.

### ***2.8 Measurement of transmembrane mitochondrial potential with DiOC<sub>6</sub>(3)***

Variations in the transmembrane mitochondrial potential ( $\Delta\Psi_m$ ) were measured with 3,3'-dihexyloxycarbocyanine iodide (DiOC<sub>6</sub>(3) (Thermo Fisher Scientific)) [41]. Adherent and non-adherent cells were pooled, and stained with DiOC<sub>6</sub>(3) (40 nM). Carbonyl cyanide m-chlorophenyl hydrazone (CCCP; Sigma-Aldrich), a potent mitochondrial oxidative phosphorylation uncoupler, was used as positive control to induce loss of  $\Delta\Psi_m$ ; to this end,

CCCP was prepared at 10 mM in DMSO (Sigma-Aldrich); CCCP (50  $\mu$ M) was added on the cells 10 min before staining with DiOC<sub>6</sub>(3). Mitochondrial depolarization is indicated by decreased green fluorescence collected through a 520/20 nm band pass filter on a Galaxy flow cytometer (Partec). Ten thousand cells were acquired; data were analysed with Flomax (Partec) or FlowJo (Tree Star Inc.) software.

### ***2.9 Measurement of reactive oxygen species production***

The overproduction of ROS was quantified by flow cytometry after staining with dihydroethidium (DHE; Thermo Fisher Scientific), which was prepared in dimethyl sulfoxide (DMSO) and used at 2  $\mu$ M. Once in the cell, DHE oxidation yields to several products, including ethidium, which exhibits an orange/red fluorescence ( $\lambda_{\text{Ex Max}}= 488$  nm;  $\lambda_{\text{Em Max}}= 575$  nm) [42, 43]. DHE mainly react with O<sub>2</sub><sup>•-</sup>. Fluorescent signal of DHE was collected with a 590 / 20 nm band pass filter. For each samples, ten thousand cells were acquired on a Galaxy (Partec) flow cytometer. Data were analyzed with FlowJo software (Tree Star Inc.).

### ***2.10 Vacuole staining with acridine orange***

The presence of autophagic vacuoles was determined by staining with acridine orange (AO) at 1  $\mu$ g/mL (15 min, 37°C). In AO-stained cells, acidic compartments (large vacuoles in autophagic cells versus small dots in non-autophagic cells) exhibit bright orange fluorescence when excited with a green light, the intensity of which is proportional to the degree of the acidity and volume of acidic vesicular organelles [39]. The nuclei were simultaneously stained with Hoechst 33342 (1  $\mu$ g/mL). At the end of the staining procedure, cells were immediately examined with an Axioskop fluorescent microscope (Zeiss). Digitized images were obtained with an AxioCam digital camera (Zeiss).

### ***2.11 Identification of autophagic vacuoles with monodansylcadaverine***

Autophagic vacuoles were also identified by fluorescence microscopy after staining with monodansylcadaverine (MDC) [44, 45]. MDC is a lysosomotropic agent which concentrates into acidic compartments by an ion trapping mechanism [46], and it is also a solvent polarity probe which increases its relative fluorescence by interacting with membrane lipids, mainly phospholipids of autophagic vacuoles [47]. Cells were seeded in 6 well plates on glass slides. MDC ( $\lambda E_x$  max 340 nm,  $\lambda E_m$  max 530 nm), prepared at 0.1 M in DMSO, was added to the culture medium at 0.1 mM. After 30 min of incubation at 37°C, glass slides were immediately examined under an Axioskop right microscope (Zeiss) by using UV light excitation. For each sample, 300 cells were examined.

### ***2.12 Cell cycle analysis***

Flow cytometric analysis of the cell cycle was realized on adherent and non-adherent cells collected by trypsinization. Cells were pooled, washed with PBS, and  $1-2 \times 10^6$  cells were stained with propidium iodide (PI) [48]. Briefly, cells were resuspended in 80% cold ethanol, washed in PBS, and resuspended in PBS containing 80  $\mu\text{g}/\text{mL}$  PI and 200  $\mu\text{g}/\text{mL}$  RNase A. After incubation (1 h, 37°C), 1-2 mL of PBS were added, and flow cytometric analyses were performed on a Galaxy flow cytometer (Partec). The parameters, forward scatter (FSC) and side scatter (SSC), were used to exclude cell debris; FSC and SSC were measured on a logarithmic scale. In addition, after gating on FSC-SSC, doublet cells were excluded by an additional gating on FL2-w (width) versus FL2-a (area); all events inside this gate correspond to single cells and were used to determine the DNA content (FL2-a). FL2a allows to measure the fluorescence of PI, which was collected using a 590/10 nm bandpass filter, and measured on a linear scale. 10,000 cells were acquired and data were analysed with Flomax (Partec) or FlowJo (Tree Star Inc.) software.

### ***2.13 Polyacrylamide gel electrophoresis and Western blotting***

Cells were lysed in a RIPA buffer and the protein concentration was measured in the supernatant using the Bicinchoninic Acid Solution (Sigma-Aldrich) [34, 35]. Seventy micrograms of proteins were diluted in loading buffer (125 mM Tris-HCl, pH 6.8, 10 %  $\beta$ -mercaptoethanol, 4.6 % SDS, 20 % glycerol, and 0.003 % bromophenol blue), separated on a polyacrylamide SDS-containing gel, and transferred onto a nitrocellulose membrane (Thermo-Scientific). After blocking nonspecific binding sites for 1 h with 5 % nonfat milk in TBST (10 mM Tris-HCl, 150 mM NaCl, 0.1 % Tween 20, pH 8), the membrane was incubated overnight with the primary antibody diluted in TBST with 1-5 % milk. The antibodies directed against caspase-3 (# 9662 Cell Signaling (Ozyme)), PARP (# 9532 Cell Signaling (Ozyme)), mTOR (# 2983 Cell Signaling (Ozyme)), Beclin-1 (# 3495 Cell Signaling (Ozyme)), Atg12 (# 4180 Cell Signaling (Ozyme)); recognizing both free Atg12 and Atg5-Atg12 complex), and LC3-I/II (# L8918 (Sigma-Aldrich)), which are rabbit antibodies, were used at 1/1000 final dilution. An antibody raised against  $\beta$ -actin (mouse monoclonal antibody; Ref: A2228 Sigma-Aldrich) was used at 1/10,000 final dilution. The membrane was washed with TBST and incubated (1 h, room temperature) with horseradish peroxidase-conjugated goat anti-mouse (Cell Signaling, # 7074) or anti-rabbit antibody (Santa-Cruz Biotechnology, # sc-2005) diluted at 1/5,000. The membrane was washed with TBST and revealed using an enhanced chemiluminescence detection kit (Supersignal West Femto Maximum Sensitivity Substrate, Thermo-Scientific) and Chemidoc XRS+ (Bio-Rad). The expression of caspase-3 (uncleaved and cleaved), PARP (uncleaved and cleaved), mTOR, Beclin 1, free Atg12, Atg12-Atg5, and the ratio LC3-II / LC3-I were calculated with Image Lab software (Bio-Rad). The expressions of caspase-3, PARP, mTOR, Beclin 1, free Atg12, and Atg12-Atg5 were normalized versus  $\beta$ -actin and expressed as normalized expression

versus control (untreated cells). The ratio LC3-II / LC3-I was calculated for each assay and expressed as fold induction versus control.

### **2.14 Statistical analysis**

Statistical analyses and determination of IC<sub>50</sub> values were done using XLSTAT software (Microsoft). Data were expressed as mean ± SD; data were considered statistically different (Mann-Whitney test) at a *P*-value of 0.05 or less.

## **3. Results and discussion**

The cytotoxic activities of compounds **1a**, **1b**, **1c**, **1d** and **1e** were evaluated in vitro on C6 cells with several complementary assays to determine i) their impact on cell growth and at the mitochondrial level, and ii) the type of cell death induced: type I (apoptosis), type II (autophagy) or type III (necrosis) [49]. The cytotoxic effects of compounds (**1a-e**) were evaluated first with the MTT assay and by crystal violet staining after 24 h of culture in a range of concentrations from 2.5 to 80 µg/mL to define IC<sub>50</sub> values for the different molecules considered. 7β-OHC was used as the positive control. With the MTT assay, which reveals mitochondrial dysfunctions and/or cell growth inhibition, and with crystal violet staining, to evaluate cell growth (cell confluency), a dose dependent decrease in the values reflecting mitochondrial activity and/or cell growth (MTT assay) as well as cell growth and cell adhesion (crystal violet) was observed with compounds **1a** and **1b**, and with 7β-OHC (**Fig. 2 A-B**). For **1a**, **1b**, and 7β-OHC, respectively, the IC<sub>50</sub> were 15.03, 77.88 and 25.03 µg/mL with the MTT assay and 80.58, 137.79 and 24.76 with crystal violet staining. The data obtained with 7β-OHC (20 µg/mL) on C6 cells are in agreement with those previously described [32]. Interestingly, the loss of cell adhesion observed by phase contrast microscopy with compounds **1a** and **1b** was associated with the lowest MTT values (**Supplementary Fig.**

1). To determine the impact of compounds **1a** and **1b** on transmembrane mitochondrial potential ( $\Delta\Psi_m$ ), the effects of two concentrations framing the  $IC_{50}$  values calculated with the MTT assay were determined. With compounds **1a** used at 10-20  $\mu\text{g/mL}$ , and **1b** used at 40-80  $\mu\text{g/mL}$ , as well as with  $7\beta\text{-OHC}$  used at 10-20  $\mu\text{g/mL}$  for 24 h, comparatively to untreated cells, a higher percentage of cells with depolarized mitochondria was observed by flow cytometry after staining with  $\text{DiOC}_6(3)$ , thus indicating the occurrence of a loss of  $\Delta\Psi_m$  under treatment with these different compounds, and side effects at the mitochondrial level (**Fig. 3 A**). With the compounds **1c**, **1d**, and **1e**, no marked effects on mitochondrial activity and cell growth were observed with the MTT assay or with crystal violet staining, respectively (**Fig. 2 C-D**). Because of the absence of cytotoxicity of compounds **1c**, **1d**, and **1e**, the corresponding  $IC_{50}$  values ( $> 80 \mu\text{g} / \text{mL}$ ) were not calculated. Thus, it appears that the cytotoxic activity is lost when the hydrogen is replaced by a hydroxyl in R1 and R3. In addition, when the hydrogen is replaced by  $\alpha\text{-OH}$  in R2, the cytotoxic activity is decreased; when it is replaced by  $\beta\text{-OH}$ , it is lost.

As compounds **1a** and **1b** inhibited cell growth, and led to a loss of  $\Delta\Psi_m$  in a range of concentrations similar to that of  $7\beta\text{-OHC}$ , which is known to have anti-gliomal activities both in vitro and in vivo [21, 22, 23], further analyses were done to characterize the type of cell death induced by these molecules. Noteworthy, on C6 cells, compounds **1a** and **1b** as well as  $7\beta\text{-OHC}$  induce an overproduction of ROS (**Fig. 3B**). With compounds **1a** and **1b**, and  $7\beta\text{-OHC}$  the ability of remaining cells to survive was also determined. To this end, the cell clonogenic survival assay was used. Interestingly, this assay brought new information and revealed marked differences between compound **1a** and **1b**, and  $7\beta\text{-OHC}$ . With **1b**, no remaining cells were able to form colonies when they had previously been treated with 20, 40 and 80  $\mu\text{g/mL}$  (**Fig. 4**). However, with **1a**, the remaining cells were able to form colonies after treatment with 20, 40  $\mu\text{g/mL}$ . At these concentrations, the aspects were similar to those in the

control and vehicle (EtOH: 0.4%) (**Fig. 4**). At 80  $\mu\text{g/mL}$ , no colonies were observed (**Fig. 4**). With 7 $\beta$ -OHC, the remaining cells were able to form colonies only after treatment with 20  $\mu\text{g/mL}$ , and the density was lower than in the control and vehicle (EtOH: 0.4%) (**Fig. 4**). Thus, whereas **1a** could be considered more effective than **1b** based on calculated  $\text{IC}_{50}$  values obtained with the MTT and crystal violet assays, the cell clonogenic survival assay revealed that **1b** was more cytotoxic since no colonies were observed at 20, 40 and 80  $\mu\text{g/mL}$  with this compound. Therefore, the anti-tumor activity of **1b** could be more promising than that of **1a** since remaining cells were unable to replicate. Thus, the cytotoxic in vitro activity determined on C6 cells can be deemed as follows: **1a** > 7 $\beta$ -OHC > **1b**. In addition, as chenodeoxycholic acid, lithocholic acid and derivatives induce cell cycle modifications and can modulate cyclin activities [50, 51, 52], the effects of compounds **1a** and **1b** as well as those of 7 $\beta$ -OHC (20-40  $\mu\text{g/mL}$ ; 24 h) on the distribution of cells in the different phases of the cell cycle were studied by flow cytometry. No difference was observed between untreated (control) and vehicle (EtOH 0.2%)-treated cells (**Fig. 5**). In agreement with previous data observed on human monocytic THP-1 cells [53], greater percentages of cells in (G2+M) were found with 7 $\beta$ -OHC (20-40  $\mu\text{g/mL}$ ) supporting a down regulation of cyclin B1 expression (**Fig. 5**). Under treatment with 7 $\beta$ -OHC, an accumulation of the cells in (G2 + M) has also been reported on the human colon cancer cell line Caco-2 [54]. Compared with control cells, no effect of compound **1a** on the distribution of cells in the different phases of the cell cycle was observed at 20 and 40  $\mu\text{g/mL}$ . With compound **1b**, whereas no modifications were detected in the distribution of cells in the different phases of the cell cycle at 20  $\mu\text{g/mL}$ , marked modifications were revealed at 40  $\mu\text{g/mL}$  (**Fig. 5**). It is therefore suggested that the double peak observed in G0/G1 might be due either to a blockage in G1 or in early S phase. As, dialkyl substituted maleic anhydrides have previously been described as Cdc 25 inhibitors [55], and as it is known that Cdc 25A is involved in the activation of the Cdk2/Cyclin E

complex, which allows progression from the G1 to S phase [56], it is therefore hypothesized that by analogy with dialkyl substituted maleic anhydrides, some steroidal maleic anhydrides, such as **1b**, could also be Cdc 25 inhibitors. This hypothesis could explain the presence of the double peak with compound **1b**. In addition, compound **1b**, was also able to significantly decrease the percentage of multiploid cells both at 20 and 40  $\mu\text{g/mL}$  (**Fig. 5**). Since our conditions of analysis by flow cytometry exclude cell debris and aggregate cells, the ability of compound **1b** to reduce multiploid cells constitutes an additional biological activity of this molecule. In addition, as compounds **1a** and **1b** could be new candidates for the treatment of malignant glioma, we attempted to determine the mode of cell death induced. After nuclear staining with Hoechst 33342, which is used to distinguish between normal cells with regular nuclei, apoptotic cells with condensed and/or fragmented nuclei, and necrotic/oncotic with altered diffused/swollen nuclei [40, 57], no apoptotic cells were observed. Mainly cells with swollen nuclei, indicating oncosis, were observed under treatment with the compound **1a**, mainly at 80  $\mu\text{g/mL}$  (**Supplementary Fig. 2**). With compound **1b**, a slight significant increase in apoptotic cells was observed but no necrotic/oncotic cells were detected (**Supplementary Fig. 2**). With 7 $\beta$ -OHC, neither oncotic, nor apoptotic cells were observed (**Supplementary Fig. 2**). Thus, in agreement with the different effects found with previous assays (MTT and crystal violet assays, measurement of the transmembrane mitochondrial potential ( $\Delta\Psi\text{m}$ ), cell cycle analysis), the different nuclear morphological changes observed with compounds **1a** and **1b** support the hypothesis that these two structurally similar molecules probably act on different cellular targets. Moreover, the induction of autophagy has been reported in various cell types treated with oxysterols, such as 7 $\beta$ -OHC, 7-ketocholesterol, 24S-hydroxycholesterol, and dendrogenine A [58, 59, 60, 61]. Therefore, as steroid molecules, such as oxysterols, have the ability to trigger lethal or survival autophagy, it was important to determine whether or not compounds **1a** and **1b** as well as 7 $\beta$ -OHC were able to induce this process. To evaluate

autophagic induction, numerous cytological and biochemical criteria are available [57]. The staining procedure with acridine orange (AO), which gives reliable data with numerous autophagic inducers (including oxysterols [60]) in different cell types, was used. In these conditions, in control and vehicle (Ethanol 0.4%)-treated cells, several small red vacuoles were observed around the nuclei (Fig. 6 A-B). In 7 $\beta$ -OHC-treated cells, mainly at 40  $\mu$ g/mL, numerous vacuoles, which were larger than in control and vehicle-treated cells, were detected. Based on the ability of 7 $\beta$ -OHC to trigger autophagy [62], these vacuoles could correspond to autophagic vesicles (Fig. 6 C-D). Under treatment with compounds **1a** and **1b**, a higher number of vacuoles, with larger sizes than in control and vehicle-treated cells, were also observed (Fig. 6 E-J). This supports the hypothesis that under treatment with compounds **1a**, **1b** and 7 $\beta$ -OHC, the lysosome is involved in cell death, and that an autophagic process could be triggered by these molecules. This hypothesis is supported by staining with mododansylcadaverin (MDC), a fluorescent probe that is incorporated into autophagic vacuoles in cultured cells by both an ion trapping mechanism and the interaction with membrane lipids. In agreement with data obtained on 7 $\beta$ -OHC-treated promonocytic U937 cells [44, 45], several C6 cells with large MDC positive vesicles were observed under treatment with 7 $\beta$ -OHC (Fig. 7); similar observations were done on C6 cells treated with compounds **1a** and **1b** (Fig. 7). Additional biochemical analyses (analysis of autophagic proteins: mTOR (Target of Rapamycin); Beclin-1; free Atg12; Atg12-Atg5 complex; determination of the LC3-II / LC3-I ratio) were performed to define the part taken by autophagy during cell death induced by the compounds **1a** and **1b**, and 7 $\beta$ -OHC [59, 62, 63]. In addition, bafilomycin (a potent inhibitor of the Vacuolar H<sup>+</sup>ATPase (V-ATPase) which controls pH in the lysosome and which also impairs fusion between autophagosome and lysosome) was used in association with the compounds **1a** and **1b**, and 7 $\beta$ -OHC to evaluate the autophagic flux [59, 63]. Western blotting analysis confirmed the absence of apoptosis

under treatment with compounds **1a** and **1b**, as well as with 7 $\beta$ -OHC (absence of cleaved caspase-3 and cleaved PARP) but revealed increased ratio of LC3-II / LC3-I, which constitutes an autophagic criteria, especially with compound **1b** and 7 $\beta$ -OHC (**Fig. 8**). With the compound **1b**, comparatively to control and vehicle (EtOH 0.4%)-treated cells, mTOR expression was higher whatever the concentration considered, Beclin-1 was slightly overexpressed especially at 20  $\mu$ g/mL, whereas free Atg-12 and the complex Atg5-Atg12 were lower (**Fig. 8**). With the compound **1a**, comparatively to control and vehicle (EtOH 0.4%)-treated cells, mTOR expression decreased in a dose dependent manner, Beclin-1 was slightly overexpressed mainly at 20 and 40  $\mu$ g/mL, and free Atg-12 was overexpressed at 40 and 80  $\mu$ g/mL whereas the complex Atg5-Atg12 was higher at 20, 40 and 80  $\mu$ g/mL (**Fig. 8**). Altogether, these data show that the cascade of autophagic events (mTOR, Beclin-1, Atg12, Atg5-Atg12, LC3-II / LC3-I) leading to the formation of the autophagosome [64] is differently affected with the compounds **1a** and **1b**, suggesting different mechanisms and/or kinetics leading to autophagy between these two molecules. Under treatment with 7 $\beta$ -OHC (used as positive control), in agreement with previous data, a strong increase of the ratio of LC3-II / LC3-I was observed [62]; this was associated with a simultaneous increase of mTOR, Beclin-1, Atg12, and Atg5-Atg12 involved in the formation of the autophagosome, mainly with 7 $\beta$ -OHC (40  $\mu$ g/mL) (**Fig. 8**). This data are in favour of the induction of autophagy with 7 $\beta$ -OHC, and supports that under treatment with this oxysterol autophagic and apoptotic induction reported on nerve cells (158N cells) are probably independent events [34, 62]. When bafilomycin was associated with 7 $\beta$ -OHC and compound **1a**, comparatively to 7 $\beta$ -OHC and compound **1a** used alone, important differences of LC3-II / LC3-I ratio were observed suggesting an autophagic flux with these two molecules (**Supplementary Fig. 3**). However, with compound **1b**, the LC3-II / LC3-I ratio is not statistically different between compound **1b** versus (compound **1b** + bafilomycin), and even slightly decreased in

(compound **1b** + bafilomycin) comparatively to compound **1b**, suggesting that **1b** does not permit the fusion between autophagosomes and lysosomes leading to autolysosomes formation (**Supplementary Fig. 3**). These data constitutes an important difference between compound **1a** and **1b**. In addition, 3-methyladenine (3-MA: 15 mM), which is an inhibitor of autophagy [65], and rapamycin (rapa: 5  $\mu$ M), which is an activator of autophagy [66], were used to determine whether 7 $\beta$ -OHC and compounds **1a** and **1b** trigger survival or lethal autophagy. It is known that 3-MA inhibits autophagy by blocking autophagosome formation via the inhibition of type III Phosphatidylinositol 3-kinases (PI-3K) [67], and that rapamycin triggers autophagy by inhibiting both mTORC1 and mTORC2 leading to the subsequent activation of Beclin-1 resulting from the inhibition of the mTOR-ULK1 pathway [66, 68]. Noteworthy, in the presence of 3-MA and rapamycin, 7 $\beta$ -OHC-induced cell death (evaluated by the percentage of floating cells in the culture medium) was strongly enhanced and strongly reduced, respectively, supporting that this oxysterol triggers a survival autophagy (**Fig. 9 A**). These data are in agreement with those obtained by Yuan et al. (2016) which reported a survival autophagy on THP-1 cells treated by a mixture of 7 $\beta$ -OHC and 7-ketocholesterol (7KC) highlighting the importance of autophagy in combating cellular stress, and cell death in atherosclerosis [69]. Currently, several studies are in favor of the activation of survival autophagy under the effect of oxysterols (7 $\beta$ -OHC, 7KC) that accumulate at the level of atheroma plaque [70, 71]. Otherwise, the ability of  $\alpha$ -tocopherol, known to prevent ROS overproduction (mainly peroxy (ROO $\bullet$ ) and alkoxy (RO $\bullet$ ) radicals) [72], strongly reduces 7 $\beta$ -OHC-induced cell death (**Fig. 9 A**). In agreement with previous investigations [73], our data obtained on C6 cells underline that 7 $\beta$ -OHC-induced ROS overproduction, known to contribute to the loss of  $\Delta\Psi_m$ , play major roles in the cell death process induced by this oxysterol. It is therefore concluded that 7 $\beta$ -OHC-induced cell death on C6 glioma cells simultaneously induces oxidative stress, loss of  $\Delta\Psi_m$ , and survival autophagy, and that the

key event leading to cell death is oxidative stress (**Fig. 10**). With compounds **1a** and **1b**, the mode of cell death observed involves mechanisms which are different from those of 7 $\beta$ -OHC. Indeed, when the cells are cultured with compounds **1a** and **1b** without or with 3-MA or rapamycin, the percentage of floating cells are similar, and in addition  $\alpha$ -tocopherol does not prevent cell death induces by these compounds whereas they enhance ROS overproduction (**Fig. 9 B-C**). Consequently, the lack of effect of  $\alpha$ -tocopherol suggests a minor role of the overproduction of ROS in cell death. Otherwise, the absence of effect of 3-MA and rapamycin on cell death suggests that if autophagy is induced by the compounds **1a** and **1b**, it does not involve conventional signaling pathways requiring the activation of PI3K and the inhibition of mTORC. It is therefore suggested that the mitochondria could play key roles in the induction of cell death with compounds **1a** and **1b** (**Fig. 10**).

Altogether, our data support that compounds **1a** and **1b** are cytotoxic molecules, with original biological characteristics. The two compounds **1a** and **1b** reduce cell growth and favour a loss of cell adhesion, induce ROS overproduction and mitochondrial dysfunctions (decreased succinate dehydrogenase activity, loss of  $\Delta\Psi_m$ ), and trigger a non apoptotic mode of cell death with characteristics of autophagy leading an increase of the ratio LC3-II / LC3-I associated with modifications of the expression of proteins (mTOR, Beclin-1, Atg12, Atg5-Atg12) involved in the formation of the autophagosome. However, only compound **1b** induced marked modifications of the cell cycle. In order to clearly establish whether the molecules **1a** and **1b** could constitute new anti-tumor drugs, additional vivo studies are required on various animal models.

In summary, novel maleic anhydride derivatives were synthesized in one step from readily available bile acids. Among these compounds, the in vitro data obtained on C6 glioma cells reveal marked cytotoxic effects with two molecules (23-(4-methylfuran-2,5-dione)-3 $\alpha$ -hydroxy-24-nor-5 $\beta$ -cholane (compound **1a**), and 23-(4-methylfuran-2,5-dione)-3 $\alpha$ ,7 $\alpha$ -

dihydroxy-24-nor-5 $\beta$ -cholane (compound **1b**)) suggesting the possibility to use steroidal maleic anhydrides as new easy-to-synthesize anti-cancer agents against tumoral cells, especially glioma cells. In addition, the data obtained on C6 cells with 7 $\beta$ -OHC support the ability of this oxysterol to induce a cell death process associated with several characteristics of survival autophagy, and bring new evidences on the ability of some sterol derivatives to induce cell death on cancer cells [74].

### **Acknowledgements**

This work was in part presented as a poster at the 8<sup>th</sup> ENOR Symposium “Oxysterols and Sterols: from Lipidomics to Food Sciences”, September 20–21, 2018, Univ. of Bologna, Bologna, Italy (<https://www.oxysterols.net/>). This work was supported by grants from: Univ. Bourgogne (Dijon, France), and Univ. El Manar (Tunis, Tunisia). Gérard Lizard is a member of the “COST Transautophagy” network. The authors acknowledge Mr Philip Bastable (Pôle Recherche – Délégation à la Recherche Clinique et Innovation – CHU Dijon, France) for english corrections.

### **Conflict of interest**

The authors declare no conflict of interest.

### **References**

- [1] E. Sievänen. Exploitation of bile acid transport systems in prodrug design. *Molecules*. 12 (2007) 1859-1889.
- [2] J.A.R. Salvador, J.F.S. Carvalho, M.A.C. Neves, S.M. Silvestr, A.J. Leitão, M.C. Silva, M.L. Sa e Melo. Anticancer steroids: linking natural and semi-synthetic compounds. *Nat Prod Rep*. 30 (2013) 324–374.

- [3] P. de Medina, M.R. Paillasse, B. Payré, S. Silvente-Poirot, M. Poirot. Synthesis of new alkylaminooxysterols with potent cell differentiating activities: identification of leads for the treatment of cancer and neurodegenerative diseases. *J. Med. Chem.* 52 (2009) 7765-7777.
- [4] M. Poirot, S. Silvente-Poirot. When cholesterol meets histamine, it gives rise to dendrogenin A: a tumour suppressor metabolite<sup>1</sup>. *Biochem. Soc. Trans.* 44 (2016) 631-637.
- [5] M.V. St-Pierre, G.A. Kullak-Ublick, B. Hagenbuch, P.J. Meier. Transport of bile acids in hepatic and non-hepatic tissues. *J. Exp. Biol.* 204(Pt 10) (2001) 1673-1686.
- [6] J.B. Gibbs, D.L. Pompliano, S.D. Mosser, E. Rands, R.B. Lingham, S.B. Singh, E.M. Scolnick, N.E. Kohl, A. Oliff. Selective inhibition of farnesyl-protein transferase blocks ras processing in vivo. *J. Biol. Chem.* 268 (1993) 7617-7620.
- [7] Y. Qian, S.M. Sebti, A.D. Hamilton. Farnesyltransferase as a target for anticancer drug design. *Biopolymers.* 43 (1997) 25-41.
- [8] X. Chen, Y. Zheng, Y. Shen. Natural Products with Maleic Anhydride Structure: Nonadrides, Tautomycin, Chaetomelic Anhydride, and Other Compounds. *Chem. Rev.* 107 (2007) 1777-1830.
- [9] E.C. Holland. Gliomagenesis: genetic alterations and mouse models. *Nat. Rev. Genet.* 2 (2001) 120-129.

- [10] S. Sathornsumetee, D.A. Reardon, A. Desjardins, J.A. Quinn, J.J. Vredenburgh, J.N. Rich. Molecularly targeted therapy for malignant glioma. *Cancer*. 110 (2007) 13-24.
- [11] M.S. Walid. Prognostic factors for long-term survival after glioblastoma. *Perm. J.* 12 (2008) 45-48.
- [12] Y.Y Xu, P. Gao, Y. Sun, Y.R. Duan. Development of targeted therapies in treatment of glioblastoma. *Cancer Biol. Med.* 12 (2015) 223-237.
- [13] J.T. Jordan, E.R. Gerstner, T.T. Batchelor, D.P. Cahill, S.R. Plotkin. Glioblastoma care in the elderly. *Cancer*. 122 (2016) 189-197.
- [14] N.A. Mohile. How I treat glioblastoma in older patients. *J. Geriatr. Oncol.* 7 (2016) 1-6.
- [15] N. Montemurro, P. Perrini, M.O. Blanco, R.Vannozzi. Second surgery for recurrent glioblastoma: A concise overview of the current literature. *Clin. Neurol. Neurosurg.* 142 (2016) 60-64.
- [16] K. Seystahl, W. Wick, M. Weller. Therapeutic options in recurrent glioblastoma-An update. *Crit. Rev. Oncol. Hematol.* 99 (2016) 389-408.
- [17] A. Cowppli-Bony, G. Bouvier, M. Rué, H. Loiseau, A. Vital, P. Lebailly, P. Fabbro-Peray, I. Baldi. Brain tumors and hormonal factors: review of the epidemiological literature. *Cancer Causes Control.* 22 (2011) 697-714.

[18] A.A. Goldberg, V.I. Titorenko, A. Beach, J.T. Sanderson. Bile acids induce apoptosis selectively in androgen-dependent and -independent prostate cancer cells. *Peer, J.* **2013**, 1:e122. doi: 10.7717/peerj.122.

[19] D. Brossard, M. Lechevrel, L. El Kihel, C. Quesnelle, M. Khalid, S. Moslemi, J.M. Reimund. Synthesis and biological evaluation of bile carboxamide derivatives with pro-apoptotic effect on human colon adenocarcinoma cell lines. *Eur. J. Med. Chem.* 86 (2014) 279-290.

[20] A. Arlia-Ciommo, V. Svistkova, S. Mohtashami, V.I Titorenko. A novel approach to the discovery of anti-tumor pharmaceuticals: searching for activators of liponecrosis. *Oncotarget.* 7 (2016) 5204-5225.

[21] M. Adamczyk, E. Scherrer, A. Kupferberg, A.N. Malviya, M. Mersel. Inhibition of p42/p44 mitogen-activated protein kinase by oxysterols in rat astrocyte primary cultures and C6 glioma cell lines. *J. Neurosci. Res.* 53 (1998) 38-50.

[22] L. Clarion, M. Schindler, J. de Weille, K. Lolmède, A. Laroche-Clary, E. Uro-Coste, J. Robert, M. Mersel, N. Bakalara. 7 $\beta$ -Hydroxycholesterol-induced energy stress leads to sequential opposing signaling responses and to death of C6 glioblastoma cells. *Biochem. Pharmacol.* 83 (2012) 37-46.

[23] C. Rakotoarivelo, M. Adamczyk, M. Desgeorges, K. Langley, J.G. Lorentz, A. Mann, D. Ricard, E. Scherrer, A. Privat, M. Mersel. 7 $\beta$ -hydroxycholesterol blocked at C-3-OH inhibits growth of rat glioblastoma in vivo: comparison between 7 $\beta$ -hydroxycholesteryl-

3beta (ester)-oleate and 7beta-hydroxycholesteryl-3-beta-O (ether)-oleyl. *Anticancer Res.* 26(3A) (2006) 2053-2062.

[24] S. Poigny, M. Guyot, M. Samadi. An expeditious synthesis of chaetomelic anhydrides A and B, and analogues. *J. Chem. Soc., Perkin Trans.1.* (1997) 2175-2177.

[25] S. Poigny, M. Guyot, M. Samadi. One-step Synthesis of Tyromycin A and Analogues. *J. Org. Chem.* 63 (1998) 1342–1343.

[26] D.H. Barton, D. Crich, W.B. Motherwell. New and improved methods for the radical decarboxylation of acids. *Chem Commun.* (1983) 939–941.

[27] G.E; Siless, M.E. Knott, M.G. Derita, S.A. Zacchino, L. Puricelli, J.A. Palermo. Synthesis of steroidal quinones and hydroquinones from bile acids by Barton radical decarboxylation and benzoquinone addition. Studies on their cytotoxic and antifungal activities. *Steroids* 77 (2012) 45-51.

[28] D.H.R. Barton, M. Samadi. The Invention of Radical Reactions. Part XXV. A Convenient Method for the Synthesis of the Acyl Derivatives of N-Hydroxypyridine-2-thione. *Tetrahedron.* 48 (1992) 7083-7090.

[29] B. Grobber, P.P. De Deyn, H. Slegers. Rat C6 glioma as experimental model system for the study of glioblastoma growth and invasion. *Cell Tissue Res.* 310 (2002) 257-270.

- [30] R.F. Barth, B. Kaur. Rat brain tumor models in experimental neuro-oncology: the C6, 9L, T9, RG2, F98, BT4C, RT-2 and CNS-1 gliomas. *J. Neurooncol.* 94 (2009) 299-312.
- [31] M. Samadi, T. Nury, A. Khalafi-Nezhad, G. Lizard. Protecting group-free radical decarboxylation of bile acids: Synthesis of novel steroidal substituted maleic anhydrides and maleimides and evaluation of their cytotoxicity on C6 rat glioma cells. *Steroids.* 125 (2017)124-130.
- [32] T. Nury, M. Samadi, A. Zarrouk, J.M. Riedinger, G. Lizard. Improved synthesis and in vitro evaluation of the cytotoxic profile of oxysterols oxidized at C4 (4 $\alpha$ - and 4 $\beta$ -hydroxycholesterol) and C7 (7-ketocholesterol, 7 $\alpha$ - and 7 $\beta$ -hydroxycholesterol) on cells of the central nervous system. *Eur. J. Med. Chem.* 70 (2013) 558-567.
- [33] L. Clarion, M. Schindler, J. de Weille, K. Lolmède, A. Laroche-Clary, E Uro-Coste, J. Robert, M. Mersel, N. Bakalara. 7 $\beta$ -Hydroxycholesterol-induced energy stress leads to sequential opposing signaling responses and to death of C6 glioblastoma cells. *Biochem. Pharmacol.* 83 (2012) 37-46.
- [34] K. Ragot, J.J. Mackrill, A. Zarrouk, T. Nury, V. Aires, A. Jacquin, A. Athias, J.P. Pais de Barros, A. Véjux, J.M. Riedinger, D. Delmas, G. Lizard. Absence of correlation between oxysterol accumulation in lipid raft microdomains, calcium increase, and apoptosis induction on 158N murine oligodendrocytes. *Biochem. Pharmacol.* 86 (2013) 67-79.
- [35] A. Zarrouk, T. Nury, E.M. Karym, A. Vejux, R. Sghaier, C. Gondcaille, P. Andreoletti, D. Trompier, S. Savary, M. Cherkaoui-Malki, M. Debbabi, A. Fromont, J.M. Riedinger, T.

Moreau, G. Lizard. Attenuation of 7-ketocholesterol-induced overproduction of reactive oxygen species, apoptosis, and autophagy by dimethyl fumarate on 158N murine oligodendrocytes. *J. Steroid Biochem. Mol. Biol.* 169 (2017) 29-38.

[36] T. Mosmann. Rapid colorimetric assay for cellular growth and survival: application to proliferation and cytotoxicity assays. *J. Immunol. Methods* 65 (1983) 55-63.

[37] V. Leoni, T. Nury, A. Vejux, A. Zarrouk, C. Caccia, M. Debbabi, A. Fromont, R. Sghaier, T. Moreau, G. Lizard. Mitochondrial dysfunctions in 7-ketocholesterol-treated 158N oligodendrocytes without or with  $\alpha$ -tocopherol: impacts on the cellular profil of tricarboxylic cycle-associated organic acids, long chain saturated and unsaturated fatty acids, oxysterols, cholesterol and cholesterol precursors. *J. Steroid Biochem. Mol. Biol.* 169 (2017) 93-110.

[38] N.A. Franken, H.M. Rodermond, J. Stap, J. Haveman, C. van Bree. Clonogenic assay of cells in vitro. *Nat. Protoc.* 1 (2006) 2315-2319.

[39] A. Altmeyer, A.C. Jung, M. Ignat, S. Benzina, J.M. Denis, J. Gueulette, G. Noël, D. Mutter, P. Bischoff. Pharmacological enhancement of autophagy induced in a hepatocellular carcinoma cell line by high-LET radiation. *Anticancer Res.* 30 (2010) 303-310.

[40] G. Lizard, S. Fournel, L. Genestier, N. Dhedin, C. Chaput, M. Flacher, M. Mutin, G. Panaye, J.P. Revillard. Kinetics of plasma membrane and mitochondrial alterations in cells undergoing apoptosis. *Cytometry* 21 (1995) 275-283.

- [41] A. Sauvat, Y. Wang, F. Segura, S. Spaggiari, K. Müller, H. Zhou, L. Galluzzi, O. Kepp, G. Kroemer. Quantification of cellular viability by automated microscopy and flow cytometry. *Oncotarget*. 6 (2015) 9467-9475.
- [42] G. Rothe, G. Valet. Flow cytometric analysis of respiratory burst activity in phagocytes with hydroethidine and 2', 7'-dichlorofluorescein. *J Leukocyte Biol* 47 (1990) 440-448.
- [43] D.C. Fernandes, J Jr Wosniak, L.A. Pescatore, M.A. Bertoline, M. Liberman, F.R. Laurindo, C.X. Santos. Analysis of DHE-derived oxidation products by HPLC in the assessment of superoxide production and NADPH oxidase activity in vascular systems. *Am J Physiol Cell Physiol*. 292 (2007) C413-422.
- [44] C. Miguet-Alfonsi, C. Prunet, S. Monier, G. Bessède, S. Lemaire-Ewing, A. Berthier, F. Ménétrier, D. Néel, P. Gambert, G. Lizard. Analysis of oxidative processes and of myelin figures formation before and after the loss of mitochondrial transmembrane potential during 7beta-hydroxycholesterol and 7-ketocholesterol-induced apoptosis: comparison with various pro-apoptotic chemicals. *Biochem Pharmacol*. 64 (2002) 527-541.
- [45] A. Vejux, S. Guyot, T. Montange, J.M. Riedinger, E. Kahn, G. Lizard. Phospholipidosis and down-regulation of the PI3-K/PDK-1/Akt signalling pathway are vitamin E inhibitable events associated with 7-ketocholesterol-induced apoptosis. *J Nutr Biochem*. 20 (2009) 45-61.
- [46] A. Niemann, A. Takatsuki, H.P. Elsässer. The lysosomotropic agent monodansylcadaverine also acts as a solvent polarity probe. *J Histochem Cytochem*. 48 (2000) 251-258.
- [47] P. Lajoie, G. Guay, J.W. Dennis, I.R. Nabi. The lipid composition of autophagic vacuoles regulates expression of multilamellar bodies. *J Cell Sci*. 118(Pt 9) (2005) 1991-2003.

- [48] A.K. Marel, G. Lizard, J.C. Izard, N. Latruffe, D. Delmas. Inhibitory effects of trans-resveratrol analogs molecules on the proliferation and the cell cycle progression of human colon tumoral cells. *Mol. Nutr. Food Res.* 52 (2008) 538-548.
- [49] P. Boya, G. Kroemer. Lysosomal membrane permeabilization in cell death. *Oncogene* 27 (2008) 6434-6451.
- [50] I. Casaburi, P. Avena, M. Lanzino, D. Sisci, F. Giordano, P. Maris, S. Catalano, C. Morelli, S. Andò. Chenodeoxycholic acid through a TGR5-dependent CREB signaling activation enhances cyclin D1 expression and promotes human endometrial cancer cell proliferation. *Cell Cycle.* 11 (2012) 2699-2710.
- [51] D. Liang, Q. Zhou, J. Zhang, W. Gong, C. Xu, B. Li, Y. Wang, J.A. Li. A novel chenodeoxycholic acid-verticinone ester induces apoptosis and cell cycle arrest in HepG2 cells. *Steroids.* 77 (2012) 1381-1390.
- [52] D. Brossard, M. Lechevrel, L. El Kihel, C. Quesnelle, M. Khalid, S. Moslemi, J.M. Reimund. Synthesis and biological evaluation of bile carboxamide derivatives with pro-apoptotic effect on human colon adenocarcinoma cell lines. *Eur. J. Med. Chem.* 86 (2014) 279-290.
- [53] H.K. Lim, H.K. Kang, E.S. Yoo, B.J. Kim, Y.W. Kim, M. Cho, J.H. Lee, Y.S. Lee, M.H. Chung, J.W. Hyun. Oxysterols induce apoptosis and accumulation of cell cycle at G(2)/M phase in the human monocytic THP-1 cell line. *Life Sci.* 72 (2003) 1389-1399.

- [54] S. Roussi, A. Winter, F. Gosse, D. Werner, X. Zhang, E. Marchioni, P. Geoffroy, M. Miesch, F. Raul. Different apoptotic mechanisms are involved in the antiproliferative effects of 7beta-hydroxysitosterol and 7beta hydroxycholesterol in human colon cancer cells. *Cell Death Differ.* 12 (2005) 128-135.
- [55] L. Brault, D. Bagrel. Activity of novel Cdc25 inhibitors and preliminary evaluation of their potentiation of chemotherapeutic drugs in human breast cancer cells. *Life Sci.* 82 (2008) 315-323.
- [56] L. Brault, M. Denancé, E. Banaszak, S. El Maadidi, E. Battaglia, D. Bagrel, M. Samadi. Synthesis and biological evaluation of dialkylsubstituted maleic anhydrides as novel inhibitors of Cdc25 dual specificity phosphatases. *Eur. J. Med. Chem.* 42 (2007) 243-247.
- [57] G. Majno, I. Joris. Apoptosis, oncosis, and necrosis. An overview of cell death. *Am. J. Pathol.* 146 (1995) 3-15.
- [58] X.M. Yuan, N. Sultana, N. Siraj, L.J. Ward, B. Ghafouri, W. Li. Autophagy Induction Protects Against 7-oxysterol-induced cell death via lysosomal pathway and oxidative stress. *J Cell Death.* 9 (2016) 1-7.
- [59] D.J. Klionsky, K. Abdelmohsen, A. Abe, M.J. Abedin, H. Abeliovich, A. Acevedo Arozena, *et al.* Guidelines for the use and interpretation of assays for monitoring autophagy (3<sup>rd</sup> edition). *Autophagy.* 12 (2016) 1-222.

- [60] T. Nury, A. Zarrouk, A. Vejux, M. Doria, J.M. Riedinger, R. Delage-Mourroux, G. Lizard. Induction of oxiaoptophagy, a mixed mode of cell death associated with oxidative stress, apoptosis and autophagy, on 7-ketocholesterol-treated 158N murine oligodendrocytes: impairment by  $\alpha$ -tocopherol. *Biochem. Biophys. Res. Commun.* 446 (2014) 714-719.
- [61] G. Segala, M. David, P. de Medina, M.C. Poirot, N. Serhan, F. Vergez, A. Mougel, E. Saland, K. Carayon, J. Leignadier, N. Caron, M. Voisin, J. Cherier, L. Ligat, F. Lopez, E. Noguier, A. Rives, B. Payré, T.A. Saati, A. Lamaziere, G. Despres, J.M. Lobaccaro, S. Baron, C. Demur, F. de Toni, C. Larrue, H. Boutzen, F. Thomas, J.E. Sarry, M. Tosolini, D. Picard, M. Record, C. Récher, M. Poirot, S. Silvente-Poirot. Dendrogenin A drives LXR to trigger lethal autophagy in cancers. *Nat Commun.* 8 (2017) 1903.
- [62] T. Nury, A. Zarrouk, J.J. Mackrill, M. Samadi, P. Durand, J.M. Riedinger, M. Doria, A. Vejux, E. Limagne, D. Delmas, M. Prost, T. Moreau, M. Hammami, R. Delage-Mourroux, N.M. O'Brien, G. Lizard. Induction of oxiaoptophagy on 158N murine oligodendrocytes treated by 7-ketocholesterol-, 7 $\beta$ -hydroxycholesterol-, or 24(S)-hydroxycholesterol: Protective effects of  $\alpha$ -tocopherol and docosahexaenoic acid (DHA; C22:6 n-3). *Steroids.* 99(Pt B) (2015) 194-203.
- [63] E. Yamada, R. Singh. Mapping autophagy on to your metabolic radar. *Diabetes.* 61 (2012) 272-280.
- [64] M. Cicchini, V. Karantza, B. Xia. Molecular pathways: autophagy in cancer – a matter of timing and context. *Clin Cancer Res.* 21 (2015) 498-504.

- [65] P.O. Seglen, P.B. Gordon. 3-Methyladenine: specific inhibitor of autophagic/lysosomal protein degradation in isolated rat hepatocytes. *Proc Natl Acad Sci U S A*. 79 (1982) 1889-1892.
- [66] D. Meng, A.R. Frank, J.L. Jewell. mTOR signaling in stem and progenitor cells. *Development*. 145 (2018) 1-16.
- [67] A. Petiot, E. Ogier-Denis, E.F. Blommaart, A.J. Meijer, P. Codogno. Distinct classes of phosphatidylinositol 3'-kinases are involved in signaling pathways that control macroautophagy in HT-29 cells. *J Biol Chem* 275 (2000) 992-998.
- [68] L. Wu, Z. Feng, S. Cui, K. Hou, L. Tang, J. Zhou, G. Cai, Y. Xie, Q. Hong, B. Fu, X. Chen. Rapamycin upregulates autophagy by inhibiting the mTOR-ULK1 pathway, resulting in reduced podocyte injury. *PLoS One*. 8 (2013) e63799.
- [69] X.M. Yuan, N. Sultana, N. Siraj, L.J. Ward, B. Ghafouri, W. Li. Autophagy induction protects against 7-oxysterol-induced cell death via lysosomal pathway and oxidative stress. *J Cell Death*. 9 (2016) 1-7.
- [70] C. He, H. Zhu, W. Zhang, I. Okon, Q. Wang, H. Li, Y.Z. Le, Z. Xie. 7-Ketocholesterol induces autophagy in vascular smooth muscle cells through Nox4 and Atg4B. *Am J Pathol*. 183 (2013) 626-637.

[71] F. Luchetti, R. Crinelli, E. Cesarini, B. Canonico, L. Guidi, C. Zerbinati, G. Di Sario, L. Zamai, M. Magnani, S. Papa, L. Iuliano. Endothelial cells, endoplasmic reticulum stress and oxysterols. *Redox Biol.* 13 (2017) 581-587.

[72] G. Rimbach, A.M. Minihane, J. Majewicz, A. Fischer, J. Pallauf, F. Virgli, P.D. Weinberg. Regulation of cell signalling by vitamin E. *Proc Nutr Soc.* 61 (2002) 415-425.

[73] A. Vejux, G. Lizard. Cytotoxic effects of oxysterols associated with human diseases: Induction of cell death (apoptosis and/or oncosis), oxidative and inflammatory activities, and phospholipidosis. *Mol Aspects Med.* 30 (2009) 153-170.

[74] M. Poirot, S. Silvente-Poirot. The tumor-suppressor cholesterol metabolite, dendrogenin A, is a new class of LXR modulator activating lethal autophagy in cancers. *Biochem Pharmacol.* 153 (2018) 75-81.

## Figure legends

**Figure 1: Synthesis of steroidal maleic anhydrides: compounds 1a, b, c, d, and e [31].**

**Figure 2: Evaluation of the cytotoxic effects of compounds 1a, b, c, d, and e, and of 7 $\beta$ -hydroxycholesterol with the MTT and the crystal violet staining assays.** After plating for 24 h, C6 rat glioma cells were cultured in the absence or presence of compounds **1a**, **1b**, **1c**, **1d**, and **1e** used at 2.5, 5, 10, 20, 40 and 80  $\mu\text{g/mL}$  (range of concentrations:  $\sim 5$  to 160  $\mu\text{M}$ ) for 24 h. Marked cytotoxic effects were only observed with compounds **1a** and **1b** and with 7 $\beta$ -OHC used as positive control (**A**, **B**); no cytotoxic effects were observed with compounds

**1c, 1d, and 1e (C, D).** Statistical analyses were realized with the Mann-Whitney test. (\*):  $P < 0.05$  or less.

**Figure 3: Evaluation of the effects of compounds 1a, and 1b on transmembrane mitochondrial potential and reactive oxygen species (ROS) production.** After plating for 24 h, C6 rat glioma cells were cultured for 24 h in the absence or presence of compounds **1a** (20-40  $\mu\text{g/mL}$ ), **1b** (40-80  $\mu\text{g/mL}$ ) and with 7 $\beta$ -OHC (positive control, 10-20  $\mu\text{g/mL}$ ) at concentrations framing the  $\text{IC}_{50}$  values. The % of cells with depolarized mitochondria was determined by flow cytometry with DiOC<sub>6</sub>(3) (**A**); the corresponding cytograms obtained by flow cytometry under different conditions of treatments are shown, and the percentages of cells with depolarized mitochondria are indicated on these cytograms. The % of ethidium positive cells (ROS overproducing cells) was determined by flow cytometry after staining with DHE (**B**). Statistical analyses were realized with the Mann-Whitney test. (\*):  $P < 0.05$  or less (assay versus vehicle). No statistically significant difference was observed between control and vehicle (EtOH (0.4%)).

**Figure 4: Cell clonogenic survival assay.** At the end of the treatments in 6-well plates with compounds **1a**, **1b** and 7 $\beta$ -OHC at 20, 40 and 80  $\mu\text{g/mL}$  for 24 h, 1,000 cells were cultured in Petri dishes for 6 days. At the beginning of the culture, the % of cells permeable to propidium iodide corresponding either to dead cells or to cells with altered cytoplasmic membranes are indicated. After 6 days of culture, the cells were stained with crystal violet to visualize cell colonies.

**Figure 5: Evaluation of the effects of compounds 1a, and 1b on the distribution of cells in the different phases of the cell cycle.** After plating for 24 h, C6 rat glioma cells were

cultured for 24 h in the absence or presence of compounds **1a**, and **1b** and with 7 $\beta$ -OHC (positive control) at 20 and 40  $\mu$ g/mL. Cell cycle analysis was realized by flow cytometry after staining with propidium iodide. Data shown are the mean of three independent experiments. Statistical analyses were realized with the Mann-Whitney test. (\*): P<0.05 or less (assay versus vehicle). No statistically significant difference was observed between control and vehicle (EtOH (0.2%)).

**Figure 6: Evaluation of the effects of compounds 1a, and 1b on the biogenesis of lysosomal vesicles evocating autophagic vesicles.** After plating for 24 h, C6 rat glioma cells were cultured for 24 h in the absence (**A, B**) or presence of compounds **1a**, and **1b** (20, 40, and 80  $\mu$ g/mL) (**E-J**) and with 7 $\beta$ -OHC (positive control; 20 and 40  $\mu$ g/mL) (**C, D**). Lysosomal vesicles, which could correspond to autophagic vesicles, were revealed by staining with acridine orange. The nuclei were counterstained with Hoechst 33342. Observations were performed by fluorescence microscopy by excitation with a green light (red fluorescence of acridine orange; active lysosomes/autophagic vesicles), a blue light (green fluorescence of acridine orange; cytoplasm) and UV light (blue fluorescence of Hoechst 33342; nuclei). The images correspond to the superposition of the three fluorescences.

**Figure 7: Evaluation of the effects of 7 $\beta$ -hydroxycholesterol and of compounds 1a, and 1b on the formation of large monodansylcadaverine positive vesicles considered as autophagic vesicles.** C6 cells were cultured for 24 h in the absence or presence of 7 $\beta$ -hydroxycholesterol (7 $\beta$ -OHC: 20 and 40  $\mu$ g/mL) and of compounds **1a** and **1b** used at 20, 40, and 80  $\mu$ g / mL. The percentage of cells with large monodansylcadaverine (MDC) positive vesicles considered as autophagic vesicles were determined. Data shown are the mean of two independent experiments realized in triplicate. Statistical analyses were realized with the

Mann-Whitney test. (\*):  $P < 0.05$  or less (assay versus vehicle). No statistically significant difference was observed between control and vehicle (EtOH (0.4%)).

**Figure 8: Evaluation of the effects of compounds 1a and 1b on caspase-3 activation, poly ADP ribose polymerase (PARP) degradation, and autophagic proteins involved in the autophagosome formation (mTOR, Beclin-1, free Atg12, Atg5-Atg12 complex, LC3-I and LC3-II).** C6 cells were cultured for 24 h in the absence or presence of compounds **1a** and **1b** used at 20, 40, and 80  $\mu\text{g} / \text{mL}$ . Apoptosis and autophagy were characterized by Western blotting with different antibodies. Apoptosis was evaluated by caspase-3 activation (cleaved caspase-3), and PARP degradation, and autophagy by (mTOR, Beclin-1, free Atg12, Atg5-Atg12 complex, LC3-I and LC3-II). The ratio LC3-II / LC3-I, which is an autophagic criteria, was determined. Data shown are representative of three independent experiments. Control: untreated cells; EtOH 0.4%: vehicle-treated cells. No difference was observed between control and the vehicle-treated cells. Statistical analyses were realized with the Mann-Whitney test. (\*):  $P < 0.05$  or less (assay versus vehicle).

**Figure 9: Evaluation of the effects of rapamycin and 3-methyladenine on cell death induced by 7 $\beta$ -hydroxycholesterol and compounds 1a and 1b.** C6 cells were cultured for 24 h in the absence or presence of 7 $\beta$ -hydroxycholesterol (20 and 40  $\mu\text{g}/\text{mL}$ ) and of compounds **1a** and **1b** used at 20, 40, and 80  $\mu\text{g} / \text{mL}$ . Alpha-tocopherol ( $\alpha$ -toco: 500  $\mu\text{M}$ ), rapamycin (rapa: 5  $\mu\text{M}$  final concentration) or 3-methyladenine (3-MA: 15 mM final concentration) were simultaneously added with compounds **1a**, **1b** or 7 $\beta$ -OHC. Data shown are representative of three independent experiments. Control: untreated cells; EtOH 0.4%: vehicle-treated cells. No difference was observed between control and the vehicle-treated

cells. Statistical analyses were realized with the Mann-Whitney test. (\*):  $P < 0.05$  or less (assay versus vehicle); (#):  $P < 0.05$  or less (assay versus (assay +  $\alpha$ -toco (or rapa, or 3-MA)).

**Figure 10: Hypothetic models of cell death on C6 glioma cells treated with 7 $\beta$ -hydroxycholesterol or compounds 1a or 1b.** On C6 rat glioma cells, with 7 $\beta$ -hydroxycholesterol (7 $\beta$ -OHC), an overproduction of ROS occurs associated with a loss of  $\Delta\Psi_m$  and survival autophagy. Indeed, 7 $\beta$ -OHC-induced cell death is prevented by rapamycin, an activator of autophagy, and it is increased by 3-methyladenine, an inhibitor of autophagy. Autophagy is characterized by increased expression of mTOR, Beclin-1, Atg12, and Atg5-Atg2. In addition, the ratio LC3-II / LC3-I is increased and strongly modified by bafilomycin which acts on the autophagic flux. Based on data observed on other cell types, it is suggested that ROS overproduction could trigger loss of  $\Delta\Psi_m$  and impact the lysosome involved in the autophagic process. This hypothesis is supported by the ability of  $\alpha$ -tocopherol to prevent 7 $\beta$ -OHC-induced side effects and cell death. Therefore, ROS could be the major event contributing in 7 $\beta$ -OHC-induced cell death. With compounds **1a** and **1b**, compound **1a** and **1b** - induced cell death is neither prevented by rapamycin, and 3-methyladenine. However, important modifications of the expression of autophagic proteins (mTOR, Beclin-1, Atg12, Atg5-Atg2, LC3-I and LC3-II) involved in the formation of the autophagosome are observed. The ratio LC3-II / LC3-I, which is mainly increased with compound **1b**, is modified by bafilomycin. No cytoprotection is observed with  $\alpha$ -tocopherol known to prevent ROS overproduction. It is therefore suggested that mitochondrial dysfunctions could be the major event contributing in compound **1a** and **1b**-induced cell death.

**Supplementary Figure 1: Evaluation of the effects of steroidal maleic anhydrides on cell growth and cell adhesion by phase contrast microscopy.** The effects of compounds **1a**

(Litho: 23-(4-methylfuran-2,5-dione)-3 $\alpha$ -hydroxy-24-nor-5 $\beta$ -cholane) and **1b** (Cheno: 23-(4-methylfuran-2,5-dione)-3 $\alpha$ ,7 $\alpha$ -dihydroxy-24-nor-5 $\beta$ -cholane) on cell growth, cell adhesion, and cell detachment of C6 glioma cells was determined by phase contrast microscopy. C6 cells were cultured for 24 h in the absence or presence of compounds **1a** and **1b** used at 20, 40, and 80  $\mu$ g / mL. Control: untreated cells; EtOH 0.1%: vehicle-treated cells. Compared to control (untreated cells) and vehicle (EtOH 0.1%)-treated C6 cells, a marked inhibition of cell growth was observed under treatment with compound 1a and 1b, and several round cells (considered as dead cells, and resulting from a loss of cell adhesion) were also detected.

**Supplementary Figure 2: Morphological characterization of steroidal maleic anhydride-induced cell death.** The mode of cell death (apoptosis/necrosis/oncosis) induced by compounds **1a** (Litho: 23-(4-methylfuran-2,5-dione)-3 $\alpha$ -hydroxy-24-nor-5 $\beta$ -cholane) and **1b** (Cheno: 23-(4-methylfuran-2,5-dione)-3 $\alpha$ ,7 $\alpha$ -dihydroxy-24-nor-5 $\beta$ -cholane) on C6 glioma cells was determined by fluorescence microscopy after nuclear staining with Hoechst 33342, which is used to distinguish between viable, apoptotic, necrotic and oncotic cells. 7 $\beta$ -hydroxycholesterol (7 $\beta$ -OHC) was used as the steroid compound of reference for cell death induction. Only apoptotic, oncotic, and normal nuclei were observed, and only the % of apoptotic and oncotic cells is shown. The morphological aspects of the nuclei of normal (living cells), apoptotic and oncotic/necrotic cells are shown; the nuclei were stained with Hoechst 33242. Data shown are the mean of two independent experiments realized in triplicate. Statistical analyses were realized with the Mann-Whitney test. (\*): P<0.05 or less (assay versus vehicle). No statistically significant difference was observed between control and vehicle (EtOH (0.4%)).

**Supplementary Figure 3: Evaluation of the autophagic flux with Bafilomycin.** C6 cells were cultured for 24 h in the absence or presence of compounds **1a** and **1b** used at 20, 40, and 80  $\mu\text{g} / \text{mL}$ , or of 7 $\beta$ -hydroxycholesterol (7 $\beta$ -OHC) used at 20 and 40  $\mu\text{g}/\text{mL}$ . Bafilomycin (100 nM) was introduced in the culture medium 20 h after the addition of compounds 1a, 1b, or 7 $\beta$ -OHC. Data shown are the mean of three independent experiments realized in triplicate. Statistical analyses were realized with the Mann-Whitney test. (\*):  $P < 0.05$  or less (assay versus vehicle); (#):  $P < 0.05$  or less (assay versus (assay + bafilomycin)). No statistically significant difference was observed between control and vehicle (EtOH (0.4%)).

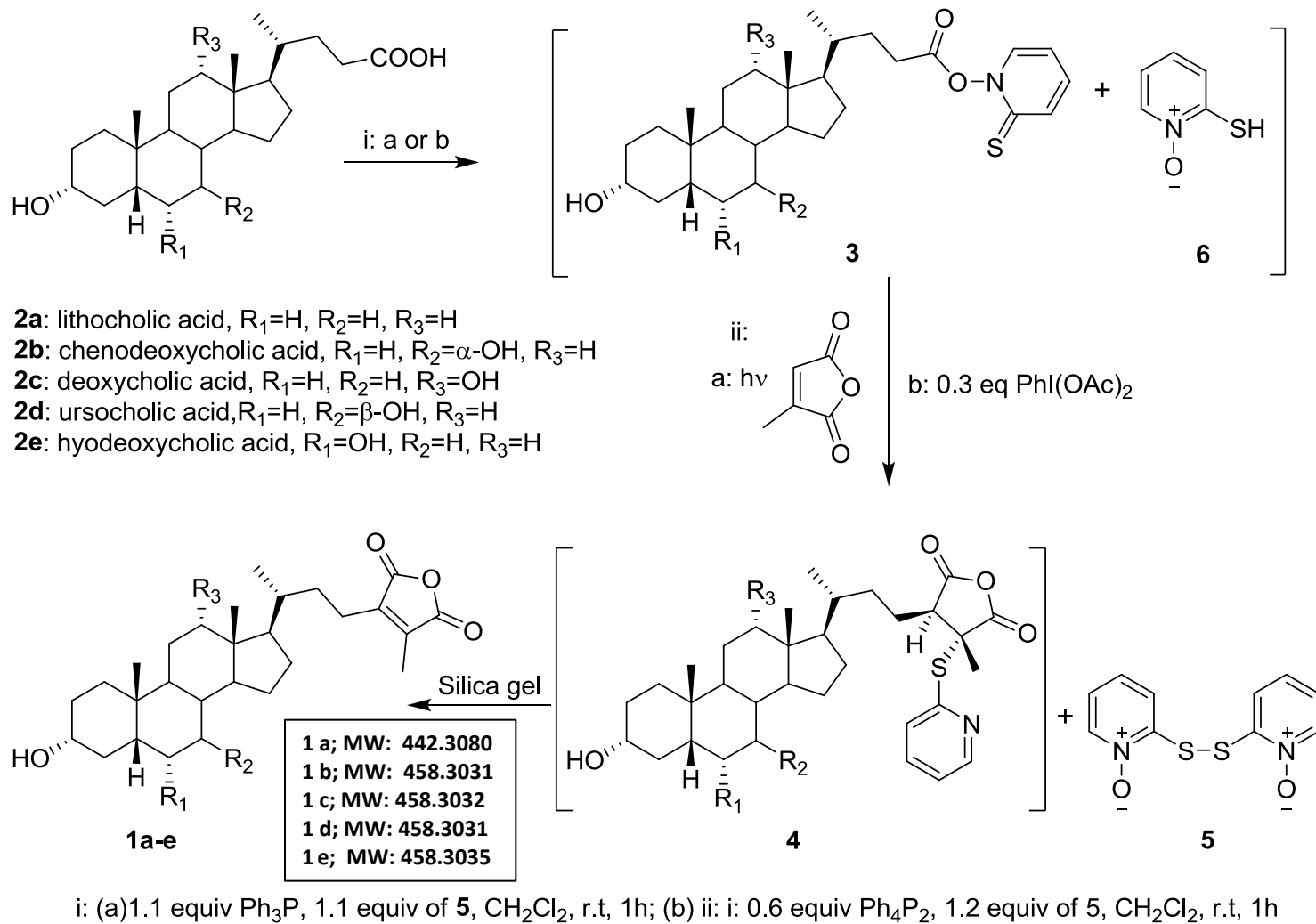


**Figure 1: Sassi K et al.**

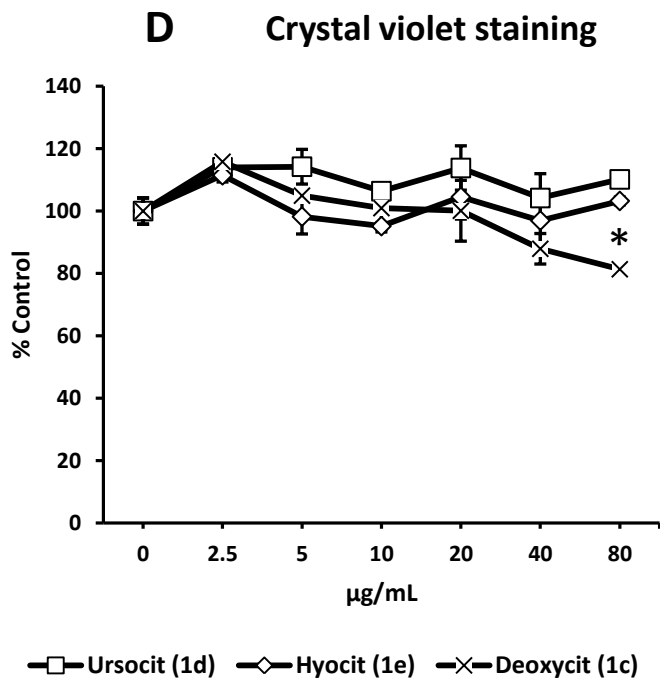
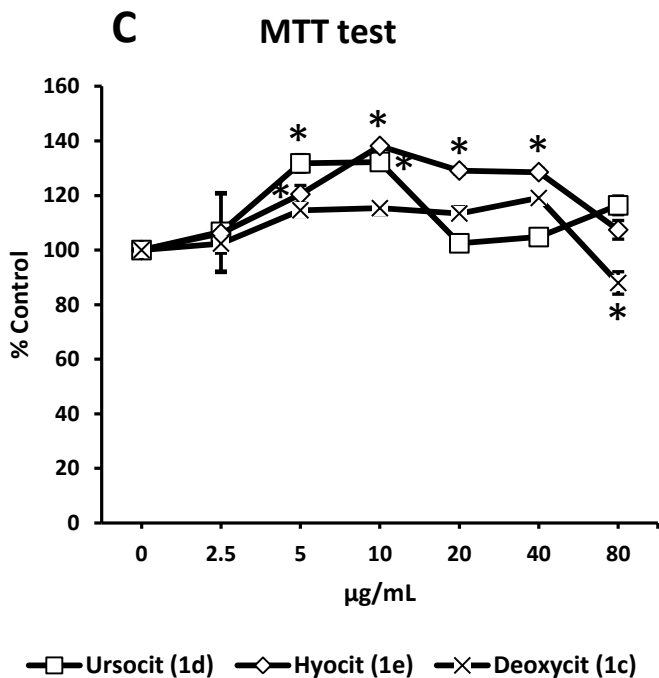
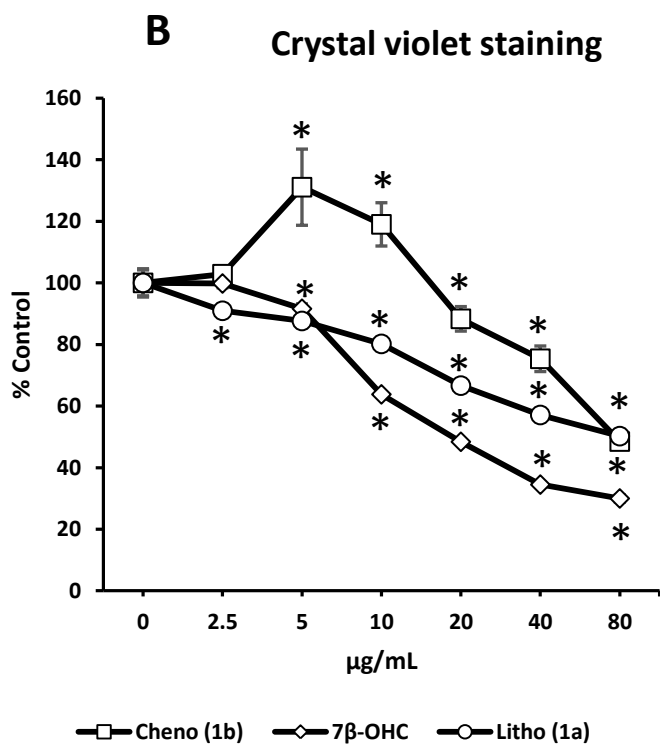
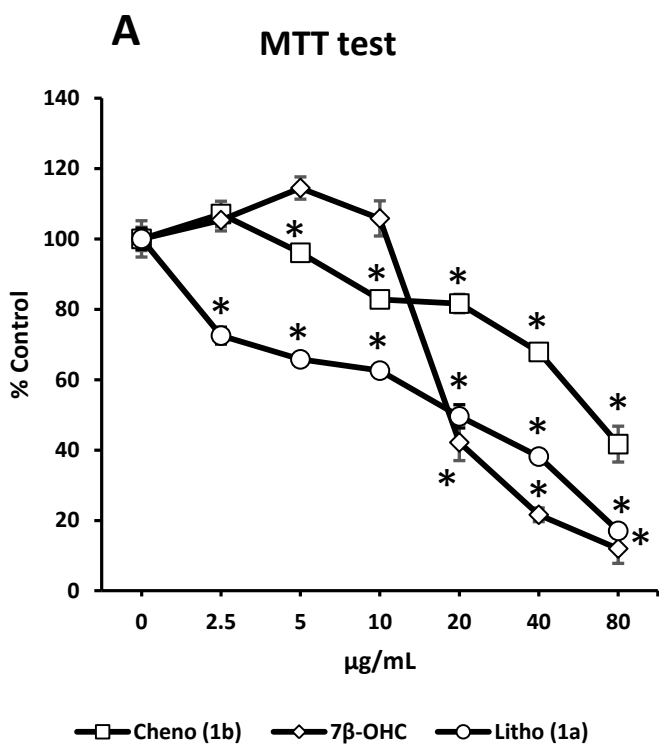
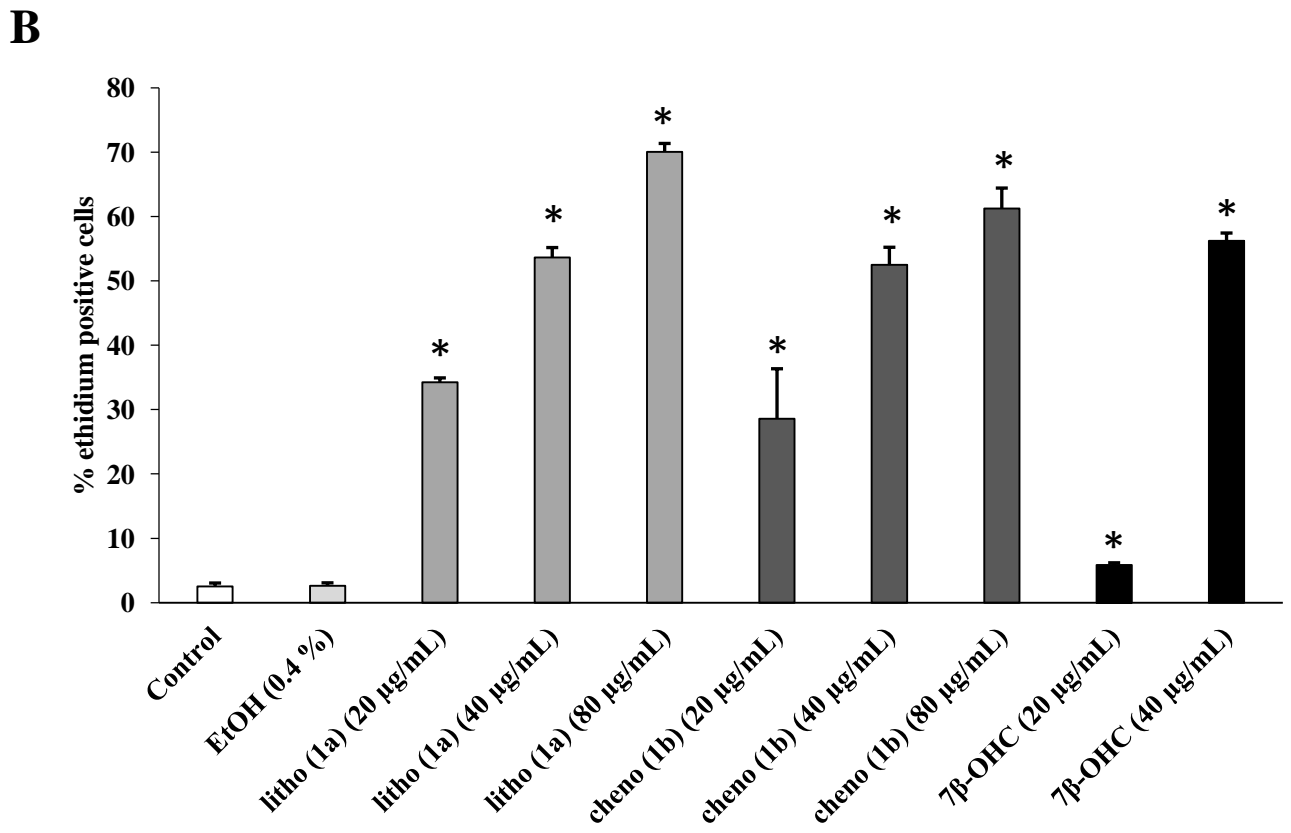
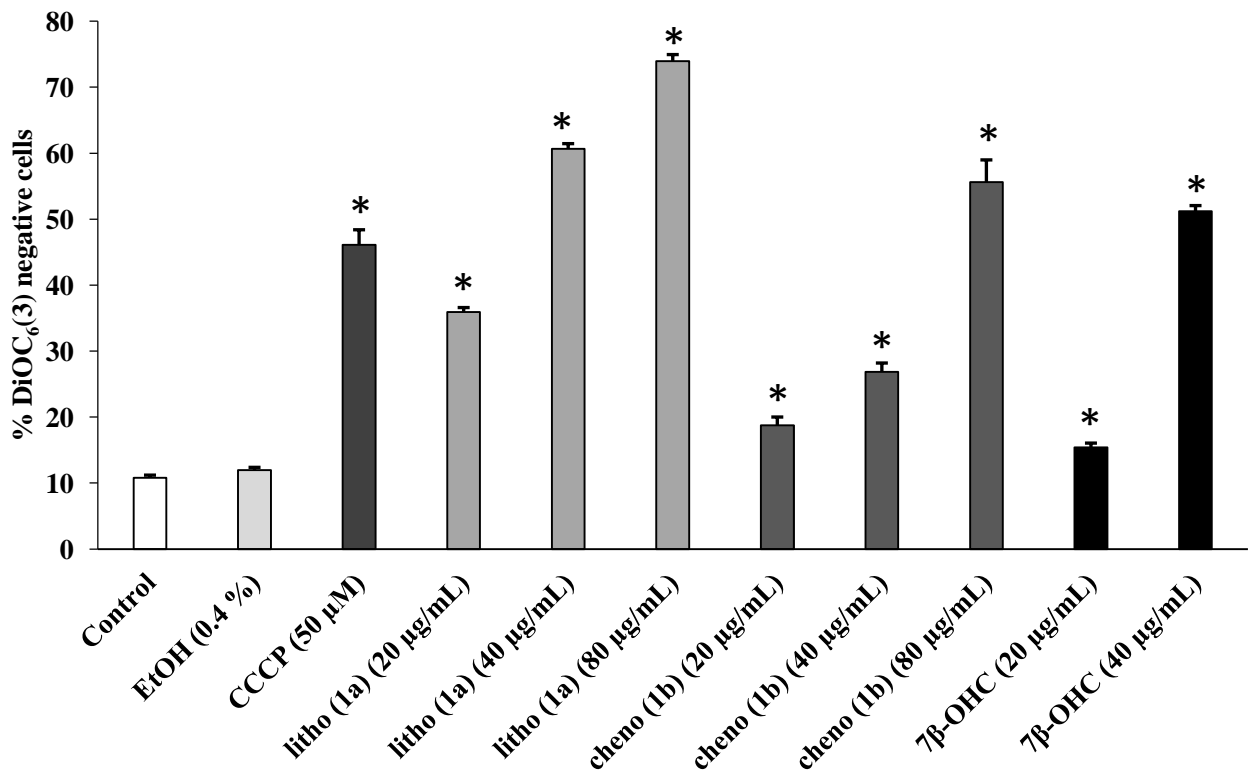
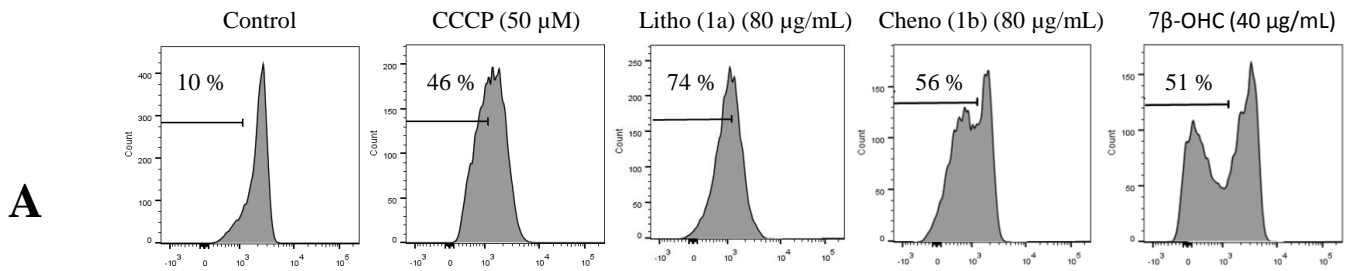


Figure 2, Sassi K et al.

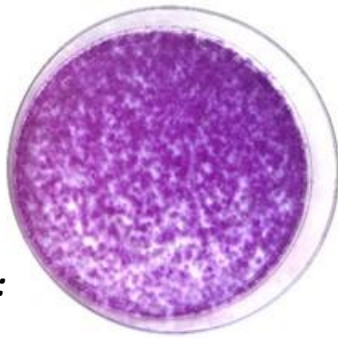


**Figure 3; Sassi K *et al.***

**Control**

**EtOH (0.4%)**

*Day 0: dead cells  
and/or  
cells with altered  
plasma membranes:*



**4%**

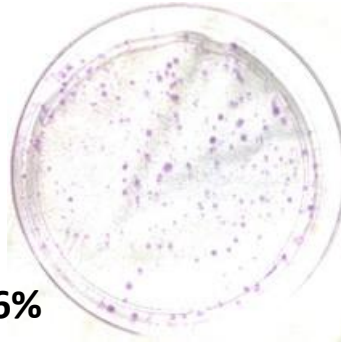
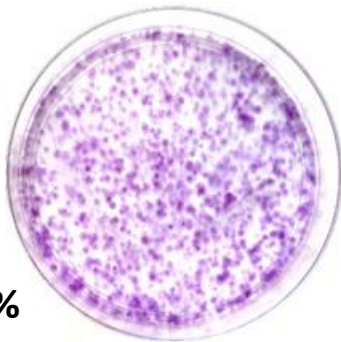
**5%**

**7 $\beta$ -OHC**

**Cheno (1b)**

**Litho (1a)**

**20  $\mu$ g/mL**

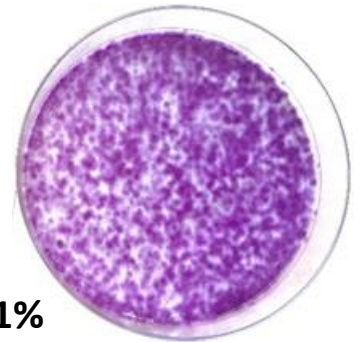
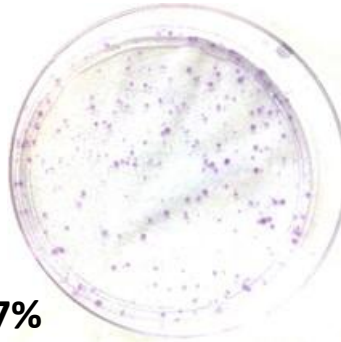
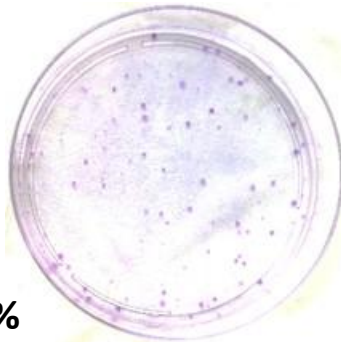


**51%**

**16%**

**7%**

**40  $\mu$ g/mL**

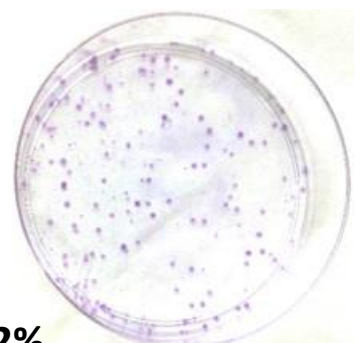
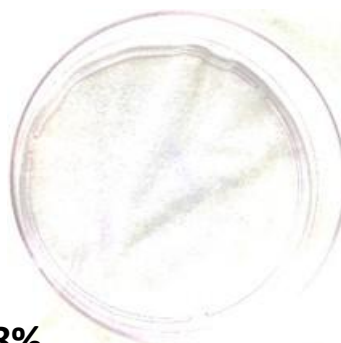
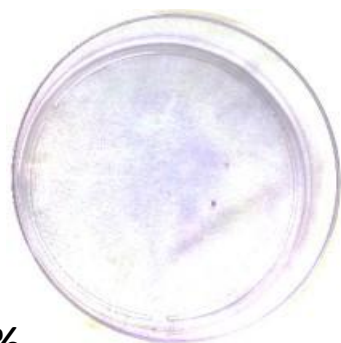


**65%**

**37%**

**21%**

**80  $\mu$ g/mL**



**92%**

**78%**

**62%**

**Figure 4; Sassi K *et al.***

	G0/G1 (%)	S (%)	G2+M (%)	Multiploid (%)
Control	45 ± 5	13 ± 1	23 ± 3	19 ± 2
EtOH (0.2 %)	44 ± 6	13 ± 1	22 ± 2	21 ± 3
Litho (1a) (20 µg/mL)	46 ± 5	11 ± 1	23 ± 1	20 ± 4
Litho (1a) (40 µg/mL)	52 ± 4	10 ± 1	22 ± 2	16 ± 2
Cheno (1b) (20 µg/mL)	56 ± 2	11 ± 1	17 ± 1	16 ± 2
Cheno (1b) (40 µg/mL) (double peak in early S phase)	47 ± 6	18 ± 1 *	18 ± 1	17 ± 4
(double peak in late G1 phase)	(62 ± 5) *	(3 ± 1)*	(18 ± 1)	(17 ± 4)
7β-OHC (20 µg/mL)	46 ± 13	3 ± 1 *	34 ± 11 *	17 ± 2
7β-OHC (40 µg/mL)	49 ± 1	9 ± 1 *	31 ± 1	11 ± 1

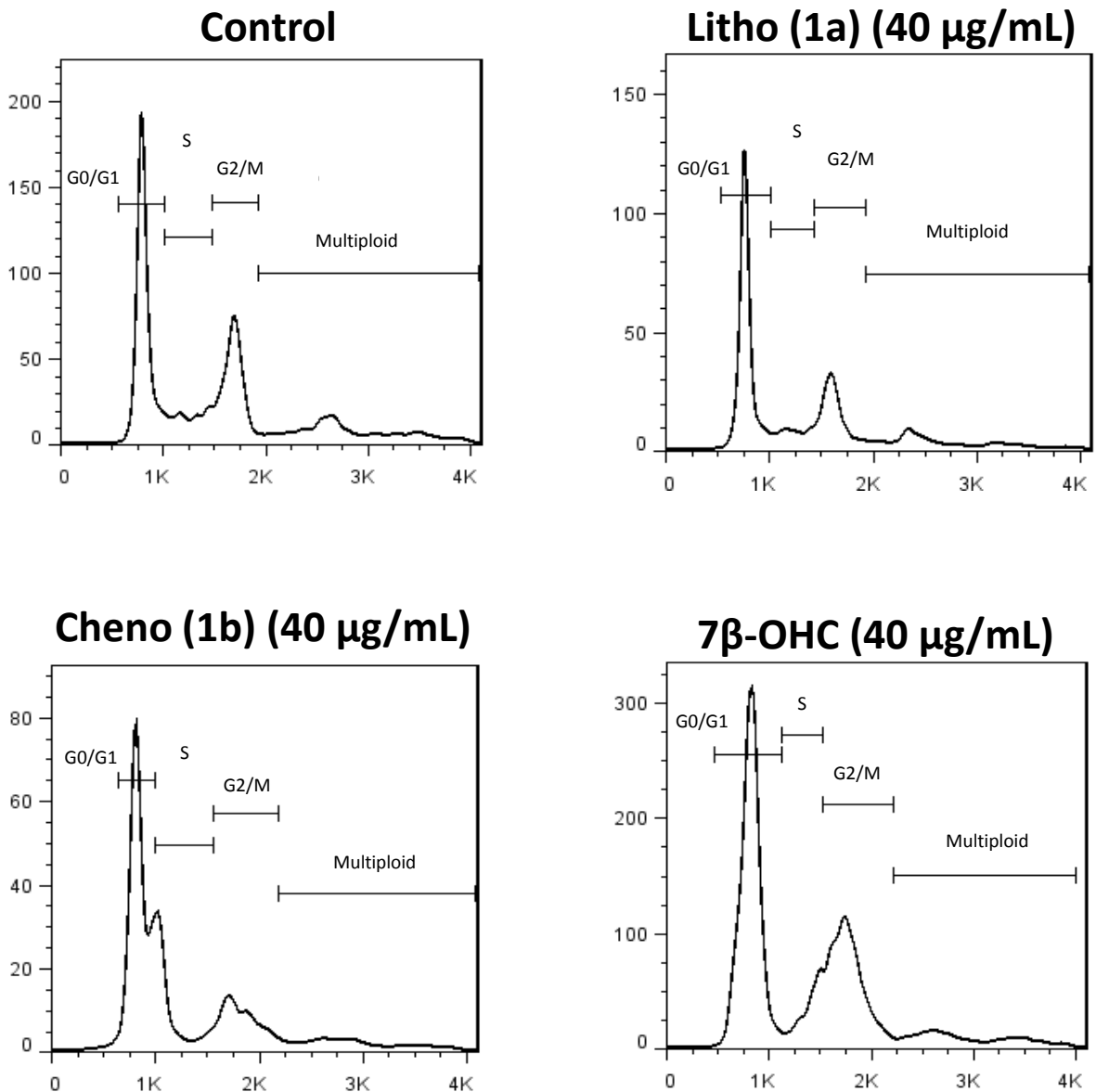


Figure 5; Sassi K *et al.*

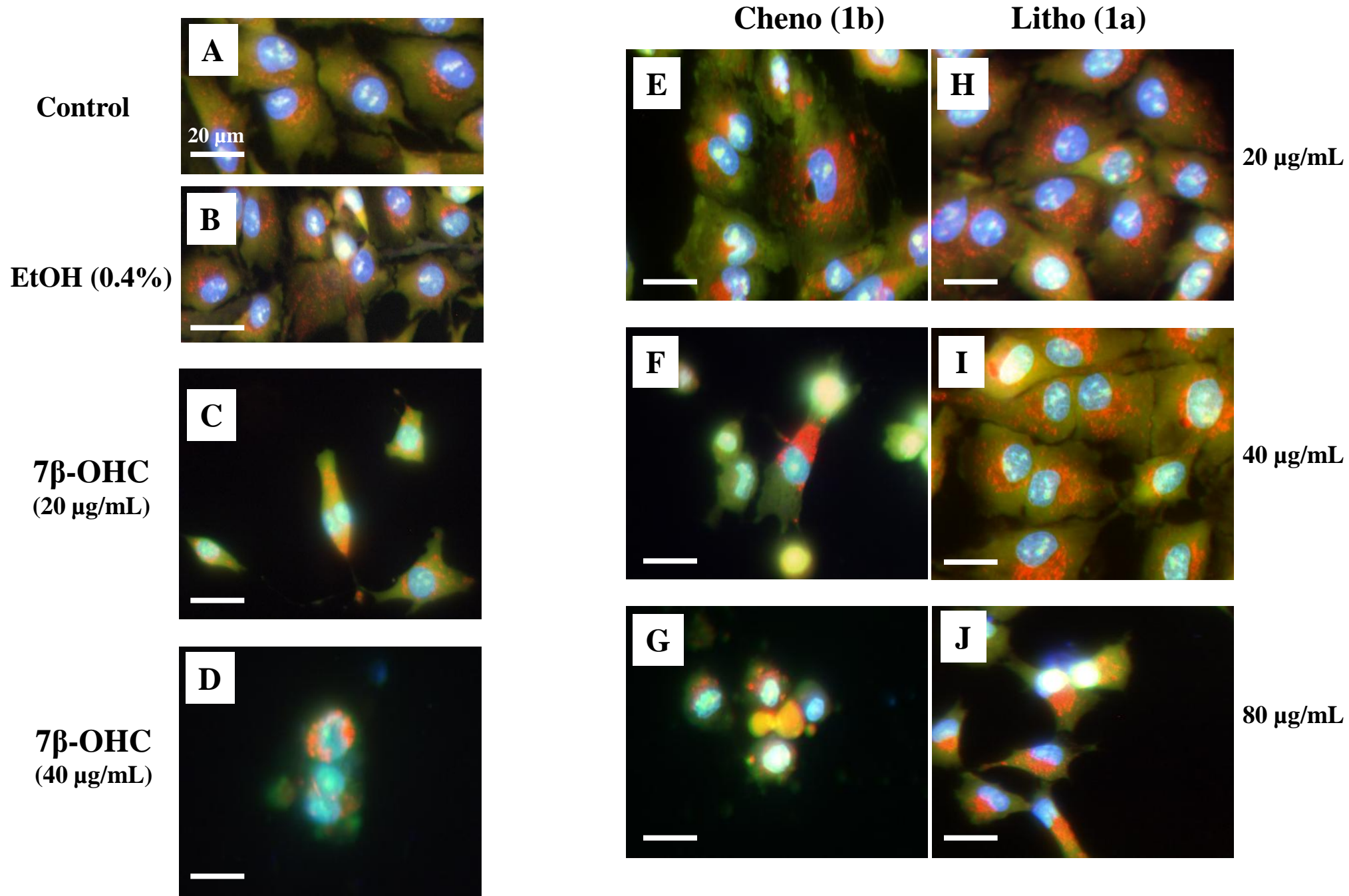
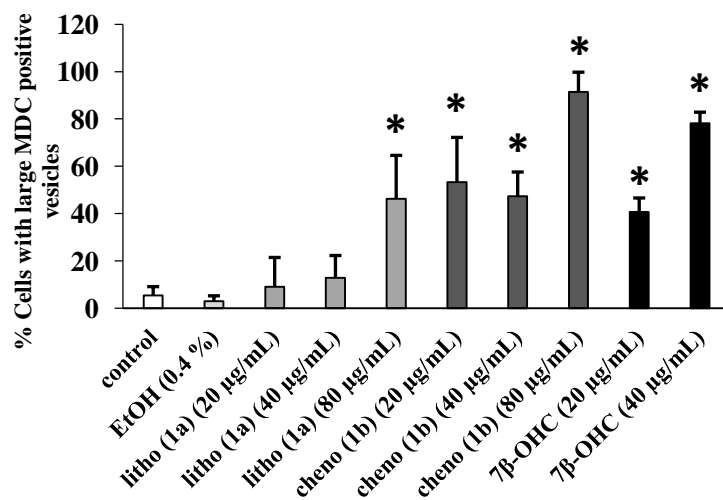
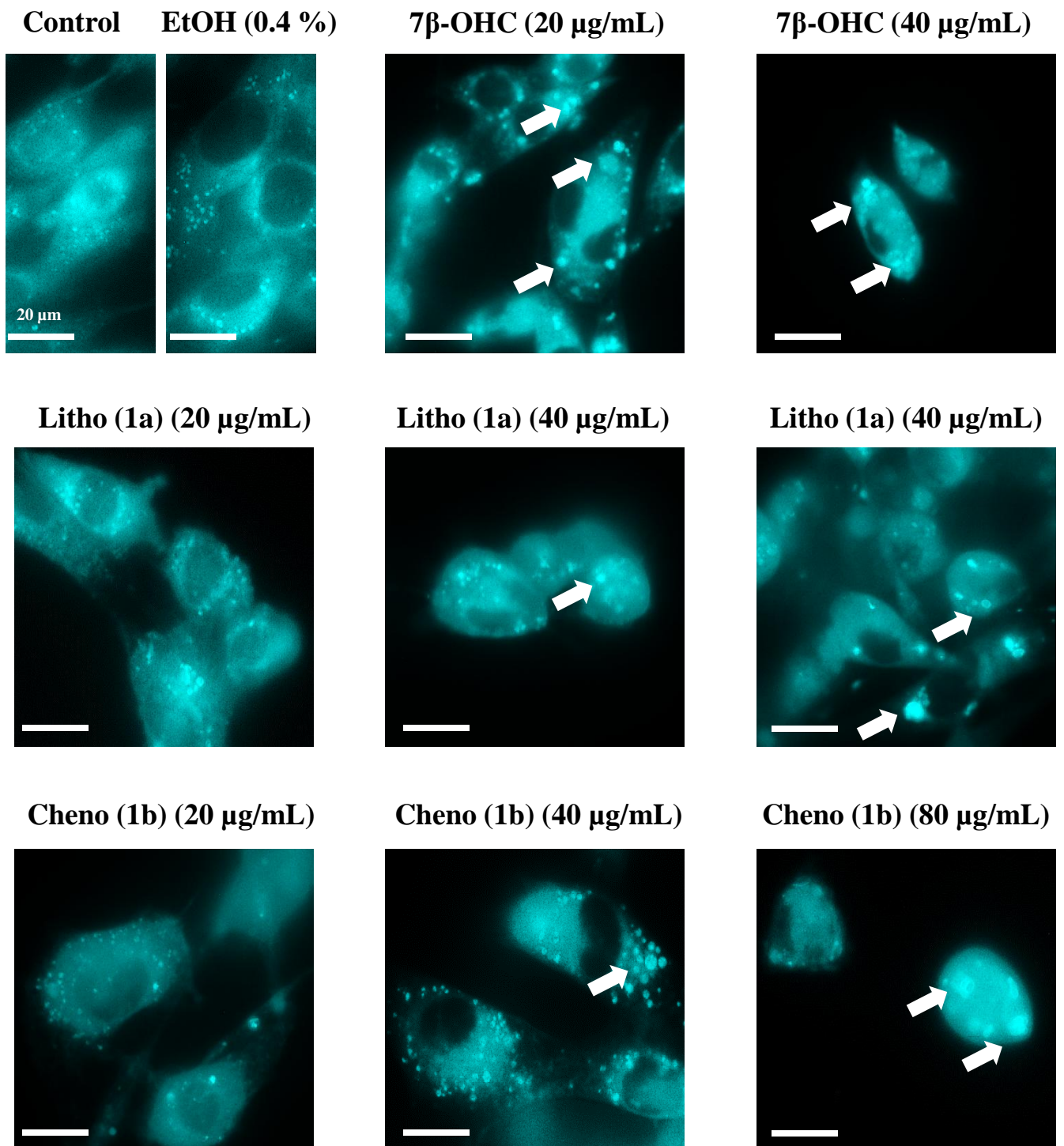


Figure 6; Sassi K *et al.*



**Figure 7; Sassi K *et al.***

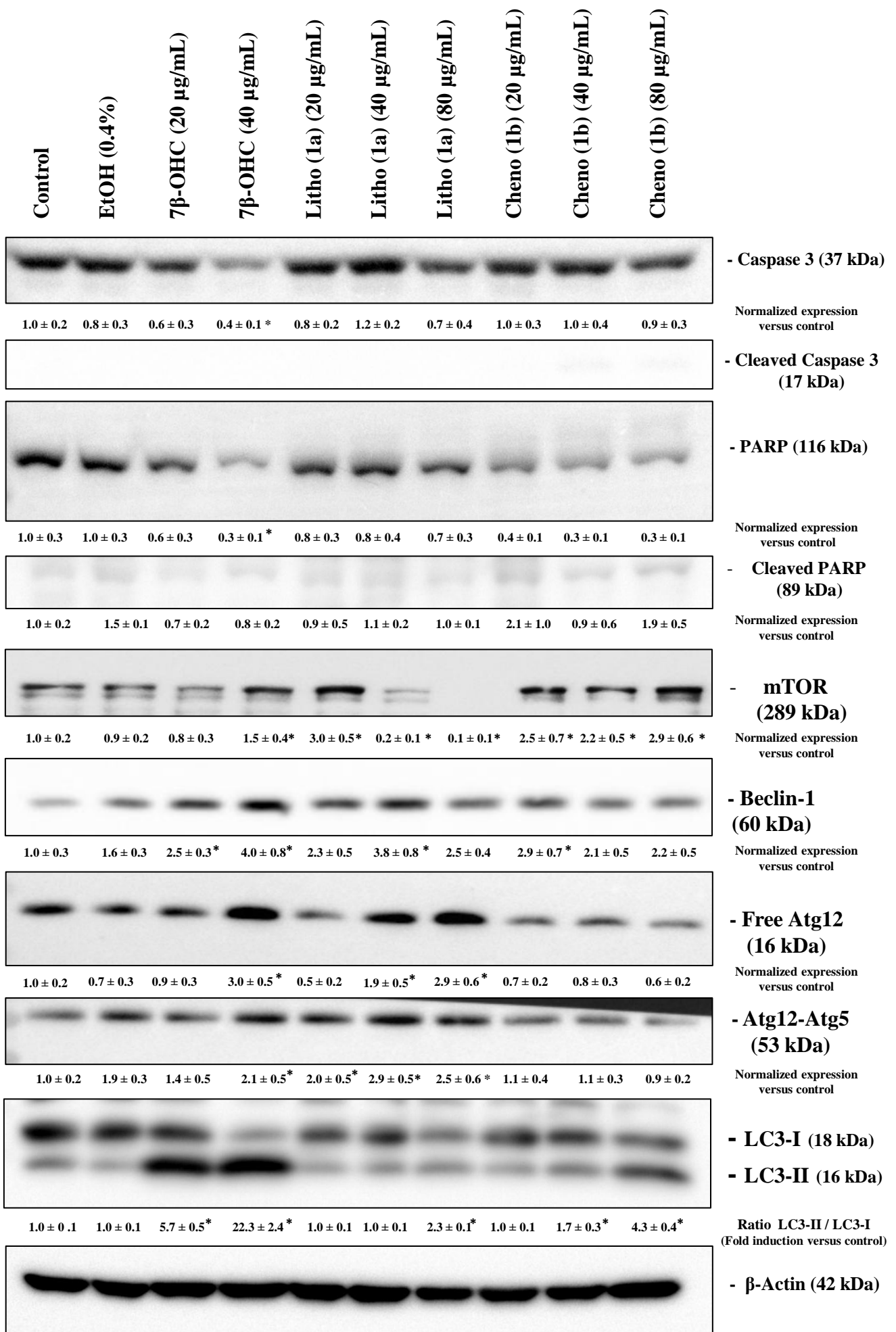
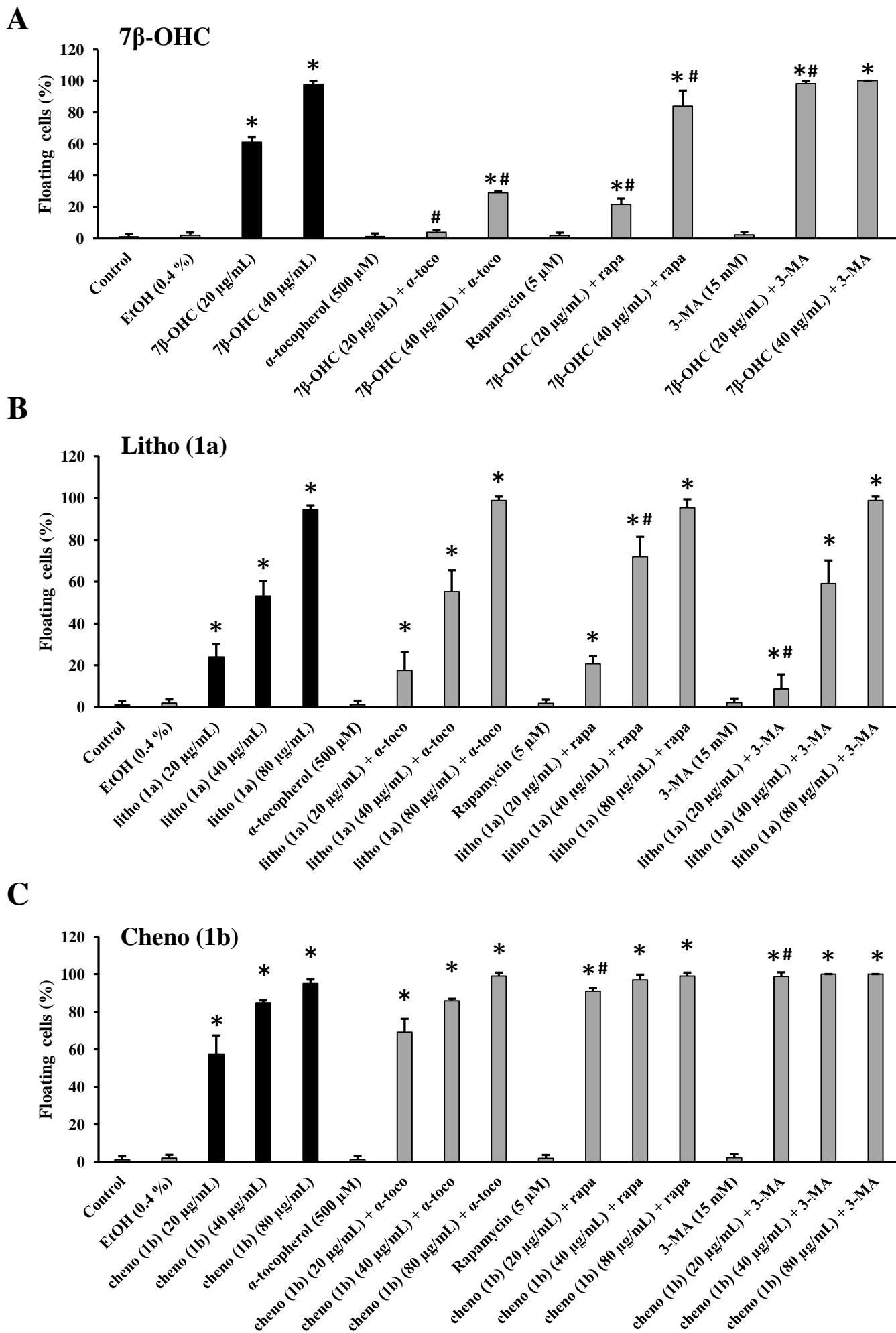
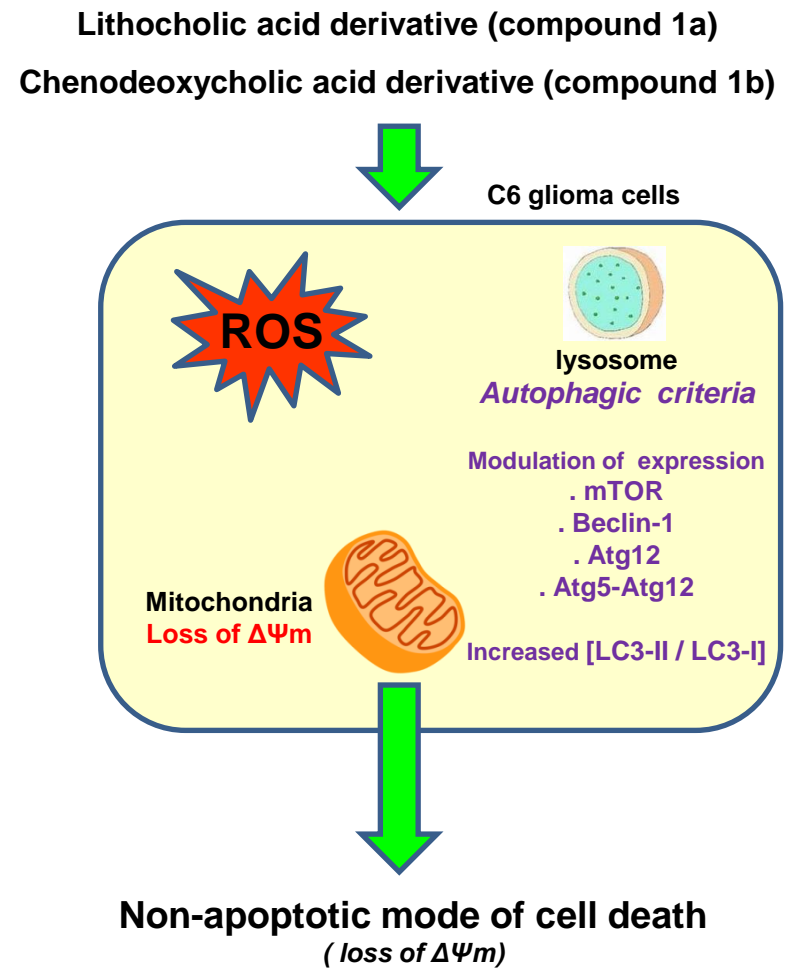
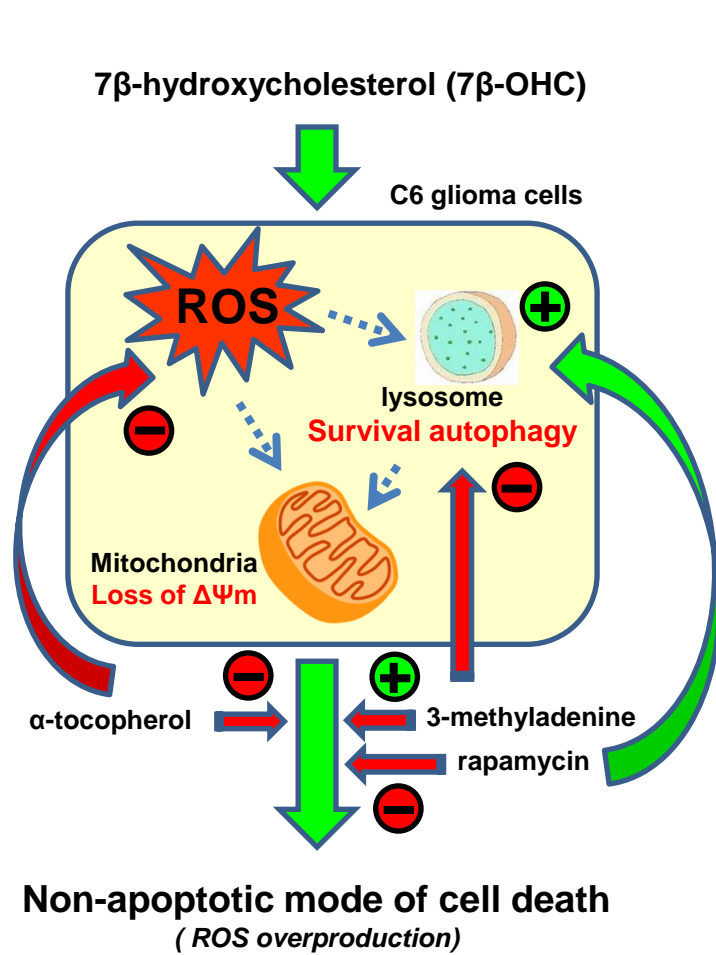


Figure 8; Sassi K *et al.*

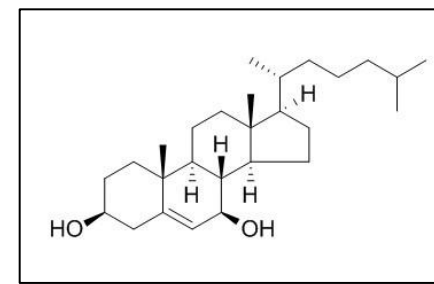
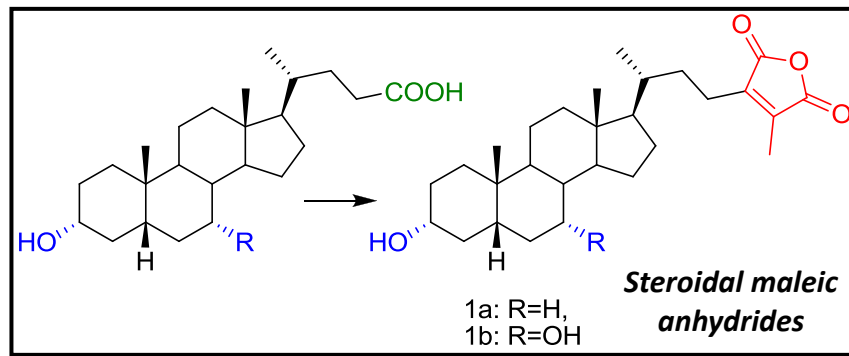


**Figure 9; Sassi K *et al.***



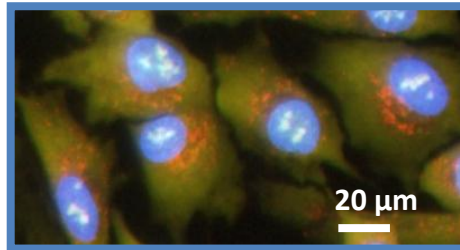
Cell death not attenuated by  $\alpha$ -tocopherol  
Cell death not modulated by 3-methyladenine and rapamycin

**Figure 10; Sassi K et al.**



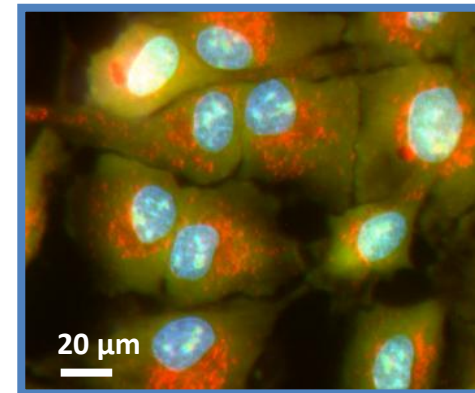
**7β-hydroxycholesterol (7β-OHC)**

2.5 – 80 μg/mL  
(5-160 μM)  
24 h



**C6 rat glioma cells**

**Cell death induction**



**Compounds (1a) and (1b) : Non apoptotic mode of cell death with several characteristics of autophagy**  
**7β-hydroxycholesterol : Non apoptotic mode of cell death associated with survival autophagy**

- cell growth inhibition
- loss of cell adhesion
- mitochondrial and lysosomal dysfunctions
- presence of acidic vacuoles (autophagic vesicles)
- cell cycle modification (with compound 1b and 7β-OHC)
- increased ratio LC3-II / LC3-I (with compounds 1a, 1b and 7β-OHC)
- modification of the expression of mTOR, Beclin-1, Atg12, Atg5-Atg12